

Regressor-Guided Image Editing Regulates Emotional Response to Reduce Online Engagement

CHRISTOPH GEBHARDT^{1,4}, ROBIN WILLARDT², SEYEDMORTEZA SADAT¹, CHIH-WEI NING¹, ANDREAS BROMBACH¹, JIE SONG³, OTMAR HILLIGES¹, AND CHRISTIAN HOLZ¹, ETH Zurich¹, UNSW Sydney², HKUST Guangzhou³, Eastern Switzerland University of Applied Sciences⁴

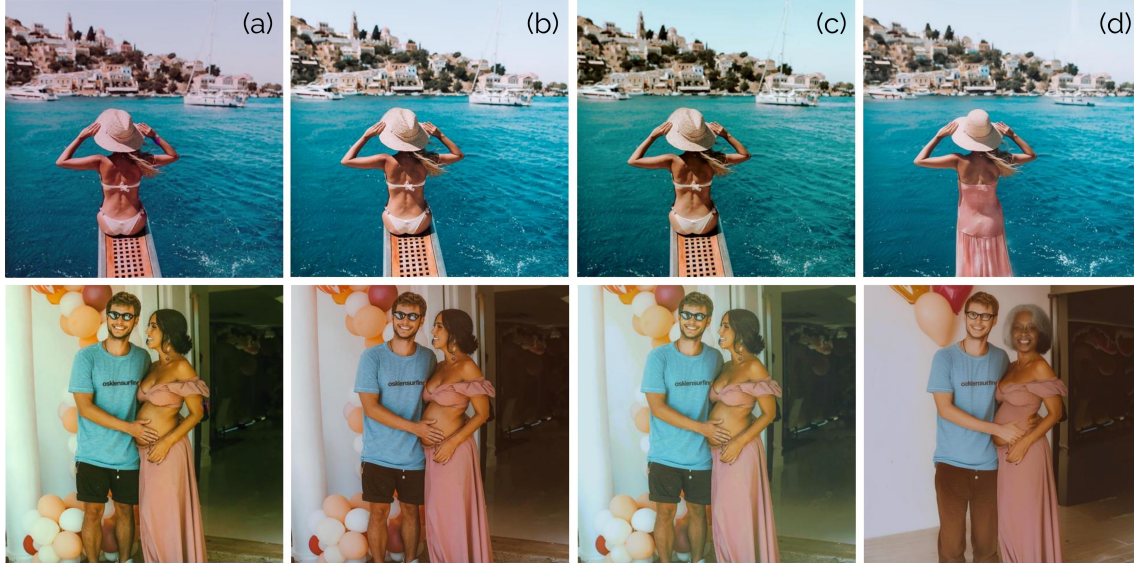


Fig. 1. We propose three regressor-guided image editing approaches aimed at reducing the emotional intensity evoked by images. These methods take the original image (b) as input and modify it using distinct strategies. The first two approaches adjust low-level properties, such as brightness, saturation, color, and sharpness, by optimizing either the style latent space of a generative adversarial network (a) or the parameters of global image transformations (c). The third approach uses score guidance and classifier-free guidance with a diffusion model to modify the image content (d). These semantic changes include adding extra layers of clothing, simplifying backgrounds, or aging the appearance of subjects. Experimental results show that the adapted images produced by the diffusion-model-based approach effectively influence viewers’ emotional responses compared to their original counterparts and, unlike greyscale images, maintain a high perceived image quality.

Emotions are known to mediate the relationship between users’ content consumption and their online engagement, with heightened emotional intensity leading to increased engagement. Building on this insight, we propose three regressor-guided image editing approaches aimed at diminishing the emotional impact of images. These include (i) a parameter optimization approach based on global image transformations known to influence emotions, (ii) an optimization approach targeting the style latent space of a generative adversarial network, and (iii) a diffusion-based approach employing classifier guidance and classifier-free guidance.

Our findings demonstrate that approaches can effectively alter the emotional properties of images while maintaining high visual quality. Optimization-based methods primarily adjust low-level properties like color hues and brightness, whereas the diffusion-based approach introduces semantic changes, such as altering appearance or facial expressions. Notably, results from a behavioral study reveal that only the diffusion-based approach successfully elicits changes in viewers’ emotional responses while preserving high perceived image quality. In future work, we will investigate the impact of these image adaptations on internet user behavior.

1 INTRODUCTION

The internet stands as one of the most significant inventions of the 20th century. Among other benefits, it democratizes access to information and facilitates unprecedented ease of communication. However, its use also yields adverse effects for users. It serves as a catalyst for addictive behaviors, for instance, tied to social media [2, 5], online gaming [112], or pornography [68]. Social media, in particular, often triggers negative emotions like dissatisfaction, envy [33], and anxiety [2]. These emotional responses can spiral into severe mental health issues such as depression [65], suicidal thoughts [2], and anorexia [106], particularly among younger users. Moreover, users consider the internet as a distraction affecting work performance [46] and well-being [20], leading to a desire to reduce their time spent online [72].

To support users in managing their internet use, various tools have been introduced through research [57, 59, 70], apps [38, 43, 102], or mobile operating systems [6]. However, this technology faces a significant limitation: The restrictions imposed by such tools are overly strict, which can lead to psychological reactance and prompt users to circumvent them [74]. Consequently, researchers suggest that effective interventions should be enforcing enough to change users' behavior without feeling too coercive [72].

Concurrently, marketing research underscores the pivotal role of emotions in shaping online behavior. Emotional experiences characterized by positive valence [40] and, to an even greater extent, heightened arousal levels [8, 84], have been shown to boost online engagement. It was also revealed that users' emotional states are influenced by the content they consume, indicating that emotions play a mediating role between content and online engagement [101, 113].

On the internet, users predominantly consume image-based content. Psychological research has highlighted how image features such as saturation or brightness can impact viewers' emotional responses [7, 63, 95]. Studies in computer vision have built upon this insight, proposing algorithms capable of manipulating images to change the emotional response of viewers [23, 88, 120].

Based on these findings, we propose generative approaches for image adaptation that regulate the emotional response of an image to decrease the time users spent online and hence facilitate a more healthy internet use. Specifically, we present three different generative image adaptation algorithms. The first approach optimizes the low-level properties of an image (e.g., brightness, contrast) to change its emotional impact. The chosen image properties are theoretically grounded, drawing from previous findings that have established their impact on eliciting emotional responses in individuals [7, 95]. The second approach uses a generative adversarial network (GAN) to disentangle content and style of an image [53] and then optimizes the style to evoke a subdued emotional response. The third approach uses a diffusion model (DM) as backbone and leverages classifier guidance (CG) as well as classifier-free guidance (CFG), to steer the denoising process of a previously inverted image to generate a similar image with reduced emotional impact.

All methods maximize the shift in the emotional impact of an image while preserving its quality and alignment to the original content. They are the first to achieve emotional image-to-image adaptation guided solely by the signal from a regressor as the information source. This regressor provides the fine-grained conditional control essential for our use case, driving images toward eliciting emotionally neutral responses. Furthermore, we are the first to demonstrate emotional image adaptation using a diffusion model, introducing classifier guidance as a tool for diffusion-based image-to-image adaptation.

Our analysis demonstrates that the proposed algorithms successfully adapt images to align more closely with the emotional reference than baseline approaches while preserving a high visual quality. Further evaluations indicate that our approaches achieve emotional property changes consistent with prior research, with notable alignment for contrast, colorfulness, and blur (other properties varied). Furthermore, all approaches successfully introduce meaningful changes

based on different emotional references, with the diffusion-based approach producing the strongest directional shifts. Qualitative inspection reveals that while the parameter optimization and the GAN latent space optimization modify color hues and brightness, the diffusion-based approach introduces semantic changes, such as altering appearance and facial expression, to align with the emotional reference.

Since our image adaptations are based on emotion-regression models, it is crucial to validate their impact on human emotional responses. Through a behavioral experiment ($N = 48$), we demonstrate that these adaptations indeed influence perceived emotions. While the parametric- and GAN-based image adaptation approaches show no emotional shifts, the diffusion-based condition results in valence ratings closer to the reference point than other approaches. It also elicits lower arousal than others, while preserving perceived image quality comparable to original images. These findings highlight the diffusion-based approach's effectiveness in altering the emotional response elicited by images, while upholding image quality.

In a follow-up experiment, we will investigate the impact of these image adaptations on social media use. Specifically, we will assess whether image adaptations also change emotions of social media users and whether these emotions cause their engagement with a social media feed to decrease.

2 RELATED WORK

Our project draws on the understanding of how image properties influence viewers' emotional responses and how these emotions, in turn, shape online behavior. Additionally, it relates to generative models for image-to-image adaptation and computational methods designed to modify images in order to modulate viewers' emotional reactions. As our goal is to help users constrain their internet use, it is also related to digital self-control tools.

2.1 The impact of image properties on emotional response

Although the personal semantic meaning of an image tends to have the strongest influence on emotional responses [54, 89], substantial evidence shows that certain image properties can also affect perceived emotions of viewers. To assess these emotional responses, researchers commonly use the Circumplex Model of Affect, which organizes emotions along two dimensions: valence, indicating the pleasantness or unpleasantness of an emotion, and arousal, representing the intensity of that emotional experience [98]. Using the terminology of this model, we will summarize key findings on how various image properties influence human emotions. Our research builds on these findings by using them to inform our computational approaches and as metrics for evaluating the generated images.

2.1.1 Color and light properties. Extensive research has explored how attributes related to color and brightness influence the emotional tone of the image. *Brightness* is generally associated with positive emotional responses and due to that also consistently preferred across various types of stimuli [105]. It has also been recognized as a universal factor influencing emotion across different cultures [39].

In terms of *color*, studies have shown that colored images, as opposed to black-and-white images, tend to evoke stronger emotional reactions. For instance, it was found that color enhances emotional valence, as measured by brain responses [21]. It was further demonstrated that unpleasant scenes presented in color are perceived as more emotionally negative and slightly more arousing compared to their grayscale counterparts [7].

Consistent with these findings, higher *saturation* levels are generally linked to more positive valence ratings. Highly saturated images not only enhance emotional valence but are generally preferred and capture greater attention, which

correlates with both valence and arousal [103]. A review paper confirms this, showing that images with more saturated colors are rated more positively across several affective image databases [95].

Regarding *contrast*, research demonstrated that enhancing contrast increases valence, while reducing contrast diminishes it. Meanwhile, the effect of contrast on arousal is relatively minor [111].

2.1.2 Structural and spatial properties. Research has also explored how the structural and spatial aspects of images influence viewers' emotional responses. Greater *variability in edge orientations* correlates with increased arousal across several commonly used affective image datasets [95]. Similarly, *smooth edges* positively impact valence, as images with angular contours are rated more negatively, while those with long, smooth contours are rated more positively [28].

Images with predominantly *low-frequency changes in color and greyscale channels*, which corresponds to broader, more gradual transitions and larger shapes, tend to evoke higher arousal, regardless of whether the image is pleasant or unpleasant [34]. Additionally, reducing resolution or introducing *blur* dampens both valence and arousal compared to sharper, intact images [32].

Symmetry, which is considered a super-principle of beauty, is generally associated with positive valence and arousal [10–12, 15, 75]. However, other studies found that while symmetry ratings correlate with valence and arousal ratings, it may be linked to lower valence ratings [95].

2.1.3 Content. It is obvious that also the content depicted in an image strongly influences viewers' emotional responses.

For example, *nudity* has been shown to increase arousal [85], while viewing *attractive faces* consistently elicits positive emotions [1, 42, 48, 108]. Additionally, *complexity* is strongly linked to heightened arousal, as more complex images offer a variety of informational cues that capture attention and stimulate greater mental energy [9].

Moreover, the *personal semantic meaning* of an image has been found to have the most significant impact on emotional responses [54, 89]. This finding aligns with appraisal theory, which suggests that individual goals and desires influence emotional reactions to external objects and events [100].

2.2 The role of emotions in online engagement

Research in marketing and psychology has explored how content influences emotions and, in turn, how these emotions affect online engagement. Studies have shown that engaging with online discussions increases emotional arousal, with higher participation rates observed when users experience positive valence [40]. In the context of brand posts, it was found that high arousal or positive valence tend to boost user engagement [113].

On the other hand, research has found that emotions of negative valence, such as anger and disgust, are the driving factors behind the rapid diffusion of false news [109]. Other work found that anger and disgust facilitate the spread of moral content due to their high-arousal nature, as low-arousal emotions of negative valence, like sadness, tend to decrease diffusion rates [17].

It was also shown that high arousal content, regardless of its valence, drives virality [8]. Similarly, studies indicate that videos eliciting high arousal are more likely to be shared, while differences in valence have minimal impact [84].

A meta-review of these and similar findings concluded that emotional arousal tends to enhance engagement behavior, while emotional valence interacts as a facilitator, modulating the extent of engagement [101].

In summary, these findings suggest that content which polarizes valence and elevates emotional arousal tends to increase online engagement levels. This aligns with the strong U-shaped correlation observed between valence and arousal in emotional databases [29, 62, 75], where extremes in valence often correspond to heightened arousal (see

Appendix A for a visualization). Informed on these insights, our approach seeks to neutralize valence and minimize arousal in adapted images, to reduce users' time spent online.

2.3 Generative models for image-to-image adaptation

Generative adversarial networks have demonstrated their capability to induce controlled changes to images across different domains [24, 25, 119]. These models have been used to adapt images in domains such as beauty [36], visual salience [78], or facial expressions [30]. Similarly, other GAN-based approaches have focused on disentangling content and style, enabling effective style translation across different content domains [53, 64].

Recently, diffusion models have surpassed GANs in terms of image synthesis quality [35, 50, 97]. These models can be fine-tuned for image-to-image translation by incorporating additional conditioning mechanisms [110, 114], enabling powerful tools like textual image editing [19].

Several works have approached image-to-image translation using DMs by guiding the inference process through a loss function applied between the generated image and the source image's representation at the same denoising step [99, 116]. Style transfer was achieved by adding noise to an input image and resampling it while conditioning the diffusion model on the reference image's style [115]. This was done by feeding the reference image's CLIP embeddings into the text-based attention mechanism guiding the diffusion process.

Most relevant to our work is a method by Mokady et al. [81]. It employs an inversion scheme for a DM scheduler [35, 104] to map images into the latent space and then optimizes the DM's null-text embedding to preserve similarity with the original image while keeping it editable within the diffusion framework.

Building on this approach, we invert images using null-text optimization to generate a noisy latent vector. We then resample the image, conditioning the diffusion model with an image caption using classifier-free guidance [51] to preserve a close resemblance to the original, while employing classifier guidance [35] to ensure the resampled image meets the criteria for neutral valence and low arousal.

2.4 Computational approaches to emotional image adaptation

Various approaches have been applied to adapt the emotional response that images elicit in viewers.

Several studies have explored the use of non-photorealistic rendering algorithms that produce stylized images to alter emotional responses [13, 83]. These works found that such algorithms tend to shift intense emotions toward a more neutral state, often due to the introduction of confusion or the loss of detail [83]. Additionally, these techniques have been shown to reduce the repulsiveness of images perceived as disgusting [13].

Early efforts in computer vision use neural networks to identify the distribution of emotions an image elicits and employ standard image transformations to change its affect towards a target emotional state [3, 88].

Another method selects a reference image based on emotional vocabulary and then optimizes the latent vectors in intermediate layers of a neural network to align an input image with this reference [4].

Various works in computer vision also used GANs to adapt the affect of images. For instance, researchers used GANs to adapt source domain images so their emotional probability distributions aligned with the target domain, enabling emotional classifiers to be applied across different datasets [117, 118]. Similarly, GAN-based style transfer techniques have been used to apply the style of an emotional reference image to an input, either globally [120] or at the object level via semantic segmentation, using multiple reference images for different objects in the scene [23].

While the approaches presented above used reference images to represent a target emotional state, other works rely on emotional classifiers or regressors to generate or adapt images based on specified sentiments. For instance,

a specialized GAN architecture has been proposed to generate emotional landscape images from noise, guided by reference values in the valence-arousal space [86]. Another approach modifies the latent noise vector of a pre-trained GAN to shift images' valence, using a regressor to verify if the desired emotional change was achieved [44].

The generative approaches proposed in this work are the first to achieve emotional image-to-image adaptation using only a regressor as the information source for the generative models. This regressor is essential to all methods, as it provides the fine-grained conditional control needed for our use case. We are also the first to demonstrate how emotional image adaptation can be achieved using a diffusion model.

2.5 Digital self-control tools

Digital self-control tools (DSCTs) are applications that help users to follow their own long-term goals by avoiding digital distractions and unwanted habitual use. These tools mostly focus on increasing productivity or reclaiming their free time [38, 43, 102]. Specialized DSCTs for parental control [92] or to avoid porn [26] are also available. Tools employ a wide range of strategies to increase self-control, e.g., hiding content on distracting websites [55], limiting functionality [80], gamification [37], or visualize time spent online [6].

Human-computer interaction (HCI) research (e.g., [60, 67, 73, 82, 90, 107]) has also investigated design patterns that help users regulate internet use, e.g., blocking distractions [57], reminding users about their long-term goals [59]. Most similar to our research, is work that leverage implicit input manipulation techniques to inhibit the natural execution of common user gestures on mobile devices to reduce the usage time [70].

However, prior work and applications mostly rely on simple decision heuristics to constrain digital media use. This often results in overly severe restrictions (e.g., turning off internet access) that trigger psychological reactance [18, 71] and, hence, are regularly circumvented [74]. This is why researchers advocate for the development of intervention mechanisms that are enforcing enough to change users' behavior without feeling too coercive [72].

Answering this call, we developed generative models that adapt images to reduce their elicited emotional intensity while ensuring a high image quality and fidelity to the originals. With this dual objective, our image adaptations have the potential to decrease the time users spent online without being overly intrusive.

3 OVERVIEW: EMOTION-REGULATING IMAGE ADAPTATION

The goal of this work is to assist users in reducing their internet consumption by regulating the emotional impact of online images. Prior studies have shown that emotionally charged experiences, characterized by polarized valence and high arousal, increase online engagement [8, 40, 84]. Moreover, computational image adaptation techniques can alter the emotions evoked in viewers [13, 83]. Concurrently, research on technologies designed to help users limit their internet use indicates that successful interventions must be sufficiently enforcing to change behavior without being overly coercive, thereby avoiding psychological reactance [72]. In the context of image adaptations, this means that the adapted images should maintain a high enough quality so that the changes are not overly pronounced or unpleasant for viewers. Additionally, we require that adaptations do not alter the image content to such an extent that the user perceives different information than what was originally presented.

Building on these insights and requirements, we establish four criteria for our image adaptation techniques (referred to as *criteria* in the following):

Approaches should (i) neutralize the valence and (ii) lower the arousal of images while (iii) preserving image quality and (iv) alignment to the original.

To achieve the desired emotional modulation, we require control beyond what existing emotional image adaptation methods offer through reference images or text-based conditioning. Therefore, we extend these approaches by employing a regressor that predicts the emotions an image elicits. This regressor guides the adjustments, enabling us to target specific emotional properties. This approach follows previous work using similar predictive models within GAN frameworks to modulate emotional properties such as valence [44].

4 METHOD

In this paper, we propose three methods to adapt images based on the outlined criteria, each varying in the degree of image modification they allow. All approaches learn adjustments using the signal of a regressor that predicts the emotions an image elicits. In the following, we first explain how we train the regressor and then detail the implementation of each approach.

4.1 Emotion regressor

We train the emotion regressor by fine-tuning a pre-trained ResNet50 model (ImageNetV2) on a custom dataset composed of multiple emotional databases. Specifically, we integrate NAPS [75], DIRTI [47], CGnA10766 [56], EmoMadrid [22], Emotion6 [88], GAPED [29], OASIS [61], OLAF [79], MAPS [45], and IAPS [62], creating a dataset of 20,460 images. We normalize valence and arousal ratings across databases to a unified scale from 0 to 1. In the appendix, we provide a figure illustrating the positions of these images within the valence-arousal space of the Circumplex Model (see Appendix A). Our regressor achieves a mean absolute error of 0.11 for valence and 0.12 for arousal on a validation split.

In alignment with *criteria* and considering the range of ratings in our dataset, we set the *emotional reference* for the adaptation approaches to a valence value of 0.5 and an arousal value of 0.

4.2 Parametric optimization

This approach optimizes parameters for differentiable image transformations to modulate the emotion response an image evokes. The advantage of this approach is its ability to adapt images of various resolutions, while the inferred parameters can also be seamlessly applied to multiple sequential frames, such as in a video [78]. By applying these global transformations, it is intentionally designed to change only the image’s low-level properties, ensuring that the depicted content remains unchanged. To ground the method theoretically, the model adapts image properties that strongly affect emotional responses (see Sec. 2.1). Specifically, we apply global image transformations that adjust the following properties: *brightness* (via exposure adjustments), *saturation* (using tone curve adjustments [78]), *color* (through color curve adjustments [52]), *contrast*, *frequency of color channel changes* (through sharpening and blurring), *blurriness*, and *symmetry* (through translation and scaling).

To satisfy *criteria*, we design the objective function to leverage the emotion regressor, facilitating image adaptation according to *emotional reference*. Additionally, we define a loss on the CLIP vectors of the input and output images to ensure their semantic similarity. CLIP is a multimodal model that learns visual concepts from natural language supervision, producing a latent space that closely aligns images depicting similar semantic concepts [93]. Figure 2 illustrates the approach.

Specifically, the objective function of the parametric optimization is defined as:

$$\arg \min_{p \in \mathcal{P}} w_1 \mathcal{L}_{\text{CLIP}}(I, T(I, p)) + w_2 \|[v', a'] - R(T(I, p))\| \quad (1)$$

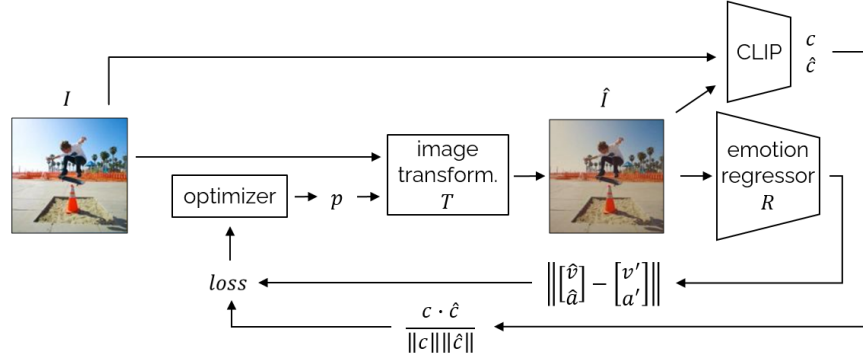


Fig. 2. Parametric optimization: To adapt an input image I , the parameters p of the differentiable image transformations T are optimized to produce a similar image that elicits a reduced emotional response, represented by $\hat{I} = T(I, p)$. The optimization minimizes the distance between the predicted valence and arousal of the adapted image, $[\hat{v}, \hat{a}] = R(\hat{I})$, and the *emotional reference*, $[v', a']$. It further ensures a high cosine similarity between the CLIP-space embeddings of the input image $c = CLIP(I)$ and the transformed image $\hat{c} = CLIP(\hat{I})$.

where p represents the optimized parameters within the feasible set \mathcal{P} , I is the input image, T is the differentiable image transformation function, R is the emotion regressor, and $[v', a']$ defines the *emotional reference*. The term $\mathcal{L}_{CLIP}(I, T(I, p)) = \frac{c \cdot \hat{c}}{\|c\| \|\hat{c}\|}$ defines the cosine similarity between the CLIP embeddings of the original image $c = CLIP(I)$ and the transformed image $\hat{c} = CLIP(\hat{I})$.

4.3 Latent style optimization

The latent style optimization uses the generator of MUNIT as its backbone to disentangle style and content of an image [53]. It then optimizes the latent style vector in alignment with our *criteria*. By modifying only the disentangled latent style, this approach is also designed to alter only low-level image features while preserving the depicted content.

To optimize the latent style according to *emotional reference*, the objective function incorporates a term that applies the emotion regressor to the adapted images. Additionally, to preserve fidelity to the original image, we employ a consistency loss between the content vector of the original and adapted images, as proposed in [53]. This approach is illustrated in Figure 3.

In the following, we explain how content and style of an image can be disentangled and define the objective function of our latent style optimization more formally.

Disentangling content and style. MUNIT employs an auto-encoder architecture as the generator in a GAN framework, allowing it to disentangle an image into a content vector and a style vector within its latent space for unsupervised style transfer across different domains. We adapt this approach by training MUNIT’s GAN on the dataset ImageNetV2 to achieve a general-purpose disentanglement of image content and style, following a methodology similar to [120]. For more details on the training process, we refer interested readers to the original MUNIT paper [53].

We trained the GAN until qualitative results confirmed effective content-style disentanglement, which was achieved after approximately 200,000 iterations. Upon completion, the generator produced an FID score of 3.2 for images generated with swapped style vectors. As demonstrated in [120], the generator successfully learned to separate high-level content features (e.g., people, chairs, cars, flowers) from low-level style characteristics (e.g., color, texture, grayscale, brightness).

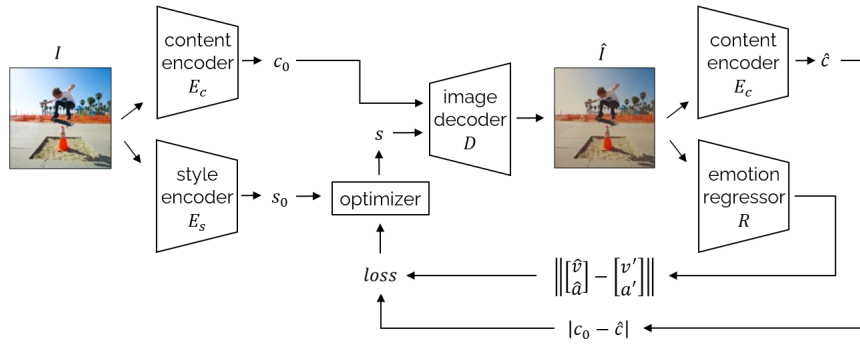


Fig. 3. Latent style optimization: To adapt an input image I , its latent style vector s is optimized to generate a similar image that elicits a reduced emotional response when decoded with I 's latent content $c_0 = E_c(I)$, resulting in $\hat{I} = D(c_0, s)$. The optimization process minimizes the distance between the predicted valence and arousal of the adapted image, $[\hat{v}, \hat{a}] = R(\hat{I})$, and the target values specified by *emotional reference*, $[v', a']$. Additionally, the optimization incorporates a term to ensure content consistency by minimizing the L1 loss between the encoded latent content of the generated image, $\hat{c} = E_c(\hat{I})$, and c_0 . The style vector s is initialized as the encoded style vector of the input image, $s_0 = E_s(I)$.

Optimization. In our optimization, we use the trained generator to disentangle the input image into content and style. We then use the style code to initialize our optimization vector, which is optimized using an objective function defined as follows:

$$\arg \min_{s \in \mathcal{S}} w_1 |E_c(I) - E_c(D(E_c(I), s))| + w_2 \left\| [v', a'] - R(D(E_c(I), s)) \right\|. \quad (2)$$

Here, R denotes the emotion regressor, $[v', a']$ specifies the *emotional reference*, I is the input image, and E_c and D are the content encoder and decoder of MUNIT, respectively. The optimized style s , within the set \mathcal{S} , is initialized as $s_0 = E_s(I)$, where E_s is MUNIT's style encoder.

4.4 Inverse diffusion with score-guided resampling

This approach leverages a diffusion model to adapt images by inverting an input image into its corresponding noise vector and then resampling it using an emotion regressor to guide the transformation towards an image that evokes a more modulated emotional response compared to the original input. By employing this method, the approach introduces flexible changes to the image, affecting not only its low-level appearance but also its high-level content.

For our implementation, we use the stable diffusion model SDXL as the backbone [91]. Additionally, we incorporate null-text optimization (NTO) to invert the input image into its corresponding latent noise vector while preserving its editability [81]. To meet *criteria*, we then denoise the latent vector using two conditioning mechanisms: (1) classifier guidance [35] to direct the denoising process towards an image aligned with neutral valence and reduced arousal; (2) classifier-free guidance [51] using the input image's caption to ensure the generated image retains the characteristics of the original input. Figure 4 illustrates this approach.

In the following, we define the three steps of our approach more formally. For a background on diffusion models and the related methods that support our approach, please refer to Appendix B.

1) *Training the guidance regressor.* To attain a regressor which we can use for CG of a diffusion model, we train a regressor R_u that predicts valence and arousal values on the output of the middle layer of a diffusion model u_t :

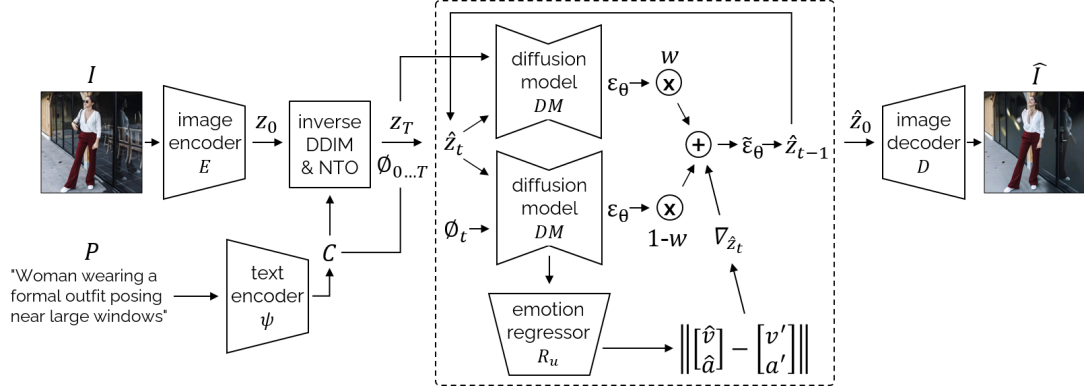


Fig. 4. Inverse diffusion with classifier-guided resampling: To adapt an input image I , it is first encoded into a latent vector $z_0 = E(I)$ and then inverted to its corresponding noise vector $z_T = DDIM_{\text{inv}}(z_0, t, C, \beta)$, while generating unconditional text embeddings for each timestep $\{\emptyset_t\}_{t=1}^T = NTO([z_T, \dots, z_0], C)$. At each step of the denoising process, \hat{z}_t is updated by blending the predicted unconditional and conditional noise ϵ_θ , further refined by a score ∇_{z_t} that quantifies alignment with the *emotional reference*. With the resulting noise vector $\tilde{\epsilon}_\theta$, \hat{z}_{t-1} can be obtained. The final latent vector \hat{z}_0 is decoded into the image $\hat{I} = D(\hat{z}_0)$, which closely resembles I while modulating the emotional response.

$[\hat{v}, \hat{a}] = R_u(u_t)$. This approach has two advantages over directly using z_t as input to the regressor. First, it is more memory-efficient, as it only requires tracing gradients through half of the diffusion model rather than the entire model during inference guidance. Second, u_t is a denser representation of the current noisy input z_t , filtering out irrelevant information and incorporating context about the current timestep t .

To train R_u , we first encode the images from our custom dataset (Sec. 4.1) into latent representations using the encoder of SDXL, $z_0 = E(I)$. We then add noise to these latents according to the forward diffusion process by randomly sampling a timestep t , resulting in $z_t = \text{ForwardDiffusion}(z_0, t, \beta)$ (see App. B.1 for a definition of β). These noisy latents, along with their corresponding timestep and the null-text embedding \emptyset , passed through the diffusion model to obtain its middle-layer output $u_t = DM_{\text{half}}(z_t, t, \emptyset)$. The output u_t is then used as input to R_u , with valence and arousal ratings from the dataset serving as prediction targets. This process is repeated until model performance stabilizes.

2) *Inverting the input image.* To adapt an image I , we first obtain its latent image encoding $z_0 = E(I)$ and the text embedding of its caption $C = \psi(\mathcal{P})$. We then perform inverse DDIM to attain an optimized noise vector $z_T = DDIM_{\text{inv}}(z_0, t, C, \beta)$. After that, we apply null-text optimization to derive unconditional embeddings for each timestep $\{\emptyset_t\}_{t=1}^T = NTO([z_T, \dots, z_0], C)$. This ensures that during inference z_t remains editable and that the resulting image stays closely aligned with the input image.

3) *Dual-conditioned resampling.* In this step, we resample \hat{z}_0 from z_T by conditioning the denoising process on the valence-arousal reference values v', a' and the caption embeddings C . During each timestep t , we condition the denoising trajectory by approximating the classifier guidance term using a score, computed as follows:

$$\nabla_{\hat{z}_t} \log p_\phi(v', a' | \hat{z}_t) = \left\| [v', a'] - R_u(DM_{\text{half}}(\hat{z}_t, t, \emptyset)) \right\| \quad (3)$$

The noise prediction process is then carried out with the modified objective:

$$\hat{\epsilon}_\theta(\hat{z}_t, t, C, \emptyset) = w \cdot \epsilon_\theta(\hat{z}_t, t, C) + (1 - w) \cdot \epsilon_\theta(\hat{z}_t, t, \emptyset) + s \cdot \nabla_{\hat{z}_t} \log p_\phi(v', a' | \hat{z}_t). \quad (4)$$

Finally, we perform the standard DDIM update step to obtain $\hat{z}_{t-1} = DDIM(\hat{z}_t, t, C, \beta)$.

In summary, from a probabilistic perspective, our approach can be interpreted as a diffusion probabilistic model $p_\theta(\hat{z}_0|z_T, \mathcal{P}, v', a')$ that generates an adapted image latent \hat{z}_0 conditioned on the noised latent vector of an input image z_T , its image caption \mathcal{P} , and specified reference values for valence v' and arousal a' .

5 IMPLEMENTATION

All approaches were implemented using PyTorch and work with images of resolution 1024x1024. Both optimization-based approaches employed the Adam optimizer with parameters $\beta_1 = 0.9$ and $\beta_2 = 0$ and a learning rate of 0.05.

For the differentiable image transformations used in the parametric optimization, we utilized existing PyTorch implementations from Kornia [96], a differentiable library of classical computer vision algorithms. Additionally, we adapted some functions from the TensorFlow implementations of the GitHub repositories of [52, 78].

For the latent style optimization, we used a high-resolution implementation of MUNIT provided by NVIDIA¹.

In our diffusion-model-based approach, we employed the Diffusers implementation of SDXL from Stability AI². Since SDXL relies on a float16 tensor representation, using default null-text optimization led to vanishing gradients. To address this, we re-implemented NTO with mixed-precision capabilities.

The network of the guidance regressor consists of four convolutional layers, each followed by ReLU activation and max-pooling, before passing through two fully connected layers to produce the final output predictions.

To attain captions for images, we leveraged the GPT4 Vision 2024-05-01-Preview model of Azure OpenAI and prompted it to provide descriptive captions that could be used as labels for a machine learning dataset.

6 EVALUATION OVERVIEW

The objective of our evaluation is to analyze if computational image adaptations that change the emotional properties of online content can be leveraged to facilitate healthy internet use by reducing the time users spent online. While previous work has shown that image manipulation impact viewer emotions (see Sec. 2.4) and that emotional content boosts online engagement (see Sec. 2.2), it is unclear if the emotional properties of images can be altered in a targeted fashion to regulate the emotions users experience and through that reduce their duration of internet use. We will address these open challenges by investigating the following two research questions:

RQ1: Can computational image adaptations effectively reduce emotional arousal and neutralize valence without compromising the quality of images?

RQ2: Do lower arousal levels and a more neutral emotional valence lead to a decreased duration of engagement with a social media feed?

We chose social media as the context for this evaluation, as it is among the most widely used services on the Internet [31] and is commonly associated with high arousal, polar valence emotional states [33, 77].

To address our research questions, we first perform a technical evaluation to assess if approaches satisfy our *criteria* in a technical sense. Subsequently, we conducted two user studies. In the first study, we assess whether our image adaptation methods can successfully reduce emotional arousal and neutralize valence in viewers while maintaining a high level of perceived image quality. In the second study, we investigate whether these emotional alterations lead to a reduced duration of engagement with a social media feed. Both user studies were preregistered on OSF [41].

¹<https://github.com/NVlabs/imaginaire>

²<https://huggingface.co/stabilityai/stable-diffusion-xl-base-1.0>

7 TECHNICAL EVALUATION

The goal of the technical evaluation is to evaluate the effectiveness of the proposed approaches in relation to our defined *criteria*. Specifically, we analyze if methods can alter valence and arousal levels as predicted by a regressor while maintaining image quality and fidelity to the original. This evaluation also examines whether these alterations cause changes in image properties in accordance with previous findings from related work. In an additional experiment, we vary the optimization objective to examine if images can be optimized toward different reference points in the valence-arousal space. Finally, we apply these approaches to adapt social media images and report the qualitative changes they induce.

7.1 Criteria alignment

In this experiment, we run different parameter configurations of our algorithms on the validation set of the COCO database [66] and compare them against the relevant metrics of our *criteria*.

7.1.1 Baselines. To evaluate the effectiveness of our developed approaches, parametric optimization, style optimization, and inverse diffusion with score-guided resampling (hereafter referred to as CG & CFG), we introduced six additional baselines, described below:

- **Original:** The original set of images without any modification or adaptation.
- **Greyscale:** The original images converted to greyscale, removing all color information. This type of filter is already available on smartphone operating systems to reduce phone use (e.g., Android’s productivity mode, Apple’s color filters).
- **Manual:** The set of static image transformations used in the parametric optimization approach applied based on parameters chosen by an expert. Parameter values were determined through experimentation on a subset of images considering the predefined *criteria*.

To analyze the contributions of different components in our diffusion-based approach, we introduced three ablated versions of the method. The variants were proposed to identify the impact of individual component of our methodology:

- **CG (Classifier Guidance Only):** This version employs the deterministic DPM Multistep Solver to invert an image [69]. Resampling is performed using only Classifier Guidance, without any text conditioning. For this baseline, we use DPM instead of DDIM as our initial experiments have shown that it produces inverted images of higher quality without NTO and (as CG is not text conditioned NTO cannot be applied).
- **NTO-instruct (Text-Conditioned Resampling Only):** In this version, images are inverted using NTO and resampled with text conditioning only, without the use of a regressor. To guide resampling, the following sentence is appended to the image caption: “*The image should elicit low arousal and neutral valence in its viewers.*”
- **NTO-edit (Text-Conditioned Resampling with Caption Refinement):** This version also uses NTO for image inversion, followed by resampling based on a modified caption. The original captions were refined by removing words or phrases likely to evoke high emotional arousal or strong positive/negative valence, ensuring a neutral emotional tone. The refined captions closely resemble the original text while avoiding words that could provoke strong emotional reactions. The modifications were generated using a GPT-4 language model.

For our diffusion-model-based baselines, we have empirically determined that a CFG scale value of 2.0 yielded the best results. This value effectively balanced introducing changes to the image while maintaining image quality and alignment to the original. For all baselines utilizing text guidance, we used the image captions provided by the

COCO database as input. Since the resolution of images in the COCO dataset is approximately 512×512 , we utilized the Diffusers implementation of Stable Diffusion from Stability AI³ as the backbone for the diffusion-model-based approaches. This also demonstrates that our approach is agnostic of the underlying diffusion model.

7.1.2 Metrics. The primary objective of this evaluation is to validate whether the proposed approaches satisfy the defined *criteria*. To this end, we employed the regressor described in Section 4.1 to estimate the valence and arousal of images. We further quantified their resemblance to the original images using the L1 loss. To evaluate image quality, we calculated the Kernel Inception Distance (KID) and the Fréchet Inception Distance (FID), both of which are widely used metrics for assessing visual quality.

Additionally, we quantified whether our approaches introduce changes to image properties in line with findings from previous research (Sec. 2.1). Thus, we measured the *colorfulness* and *saturation* of images using metrics proposed by Hasler and Suesstrunk [49]. The mean *brightness* of images was computed following the metric introduced by Goetschalckx et al. [44]. *Contrast* was calculated as described by Peli [87] and blur was assessed using the no-reference perceptual blur metric proposed by Crete et al. [27]. To quantify the *variability in edge orientations*, we followed the study by [94] and computed the first order entropy of edge orientations. To analyze *low-frequency changes in color and greyscale channels*, we computed Z-score transformed wavelet coefficients for both RGB and grayscale images using the methodology proposed by Delplanque et al. [34]. We quantified left-right mirror *symmetry* in images using the approach of Brachmann and Redies [14], leveraging filter responses of a convolutional neural network (VGG16) to capture color, edges, texture, and higher-order symmetry. Note that we omitted quantifying *edge smoothness* as proposed in [28] due to the excessive manual effort required to label all significant contours in an image.

7.1.3 Results. Our approaches share a dual-objective design: one objective ensures that the adapted images remain similar to the original, while the other introduces changes to neutralize the valence and reduce the arousal evoked in viewers. To understand the changes our approaches introduce to images, we fixed the weight of the similarity-preserving objective ($w_1 = 1.0$ for parametric optimization and style optimization, and $w = 2.0$ for CG & CFG and CG) and systematically varied the weight of the emotional adaptation objective ($w_2 \in \{0.1, 0.3, 0.5, 0.7, 1.0\}$ for parametric optimization and style optimization, and $s \in \{0.05, 0.1, 0.2, 0.3, 0.4\}$ for CG & CFG and CG). In the following, we first present the quantitative results of this experiment, followed by the qualitative findings.

Criteria alignment. Figure 5 illustrates how the metrics evolve as the weights of the emotional adaptation objective are adjusted. The results demonstrate that, in line with our *criteria*, all approaches effectively neutralize valence (Fig. 5a) and lower arousal (Fig. 5b) compared to the original images. An exception is NTO-edit, which does not produce lower valence values relative to the original images. To formally confirm this observation, we fitted ordinary least squares (OLS) regression models to the differences between the valence and arousal values of the original images and their adapted counterparts for each weight configuration of parametric optimization, style optimization, CG, and CG & CFG.

For valence, the OLS models for all approaches were statistically significant ($p < 0.03$), indicating that higher weights in the emotional adaptation objective were strongly associated with reductions in valence. The predictor term (β_1) for each approach was as follows: style optimization ($\beta_1 = -0.0121$, $p = 0.022$), parametric optimization ($\beta_1 = -0.0220$, $p = 0.018$), CG ($\beta_1 = -0.0960$, $p < 0.001$), and CG & CFG ($\beta_1 = -0.0401$, $p = 0.001$). The observed negative relationships are attributable to the original images having a positive average valence, with increasing weight on the emotional adaptation objective driving them toward the *emotional reference*.

³<https://huggingface.co/stabilityai/stable-diffusion-2-1-base>

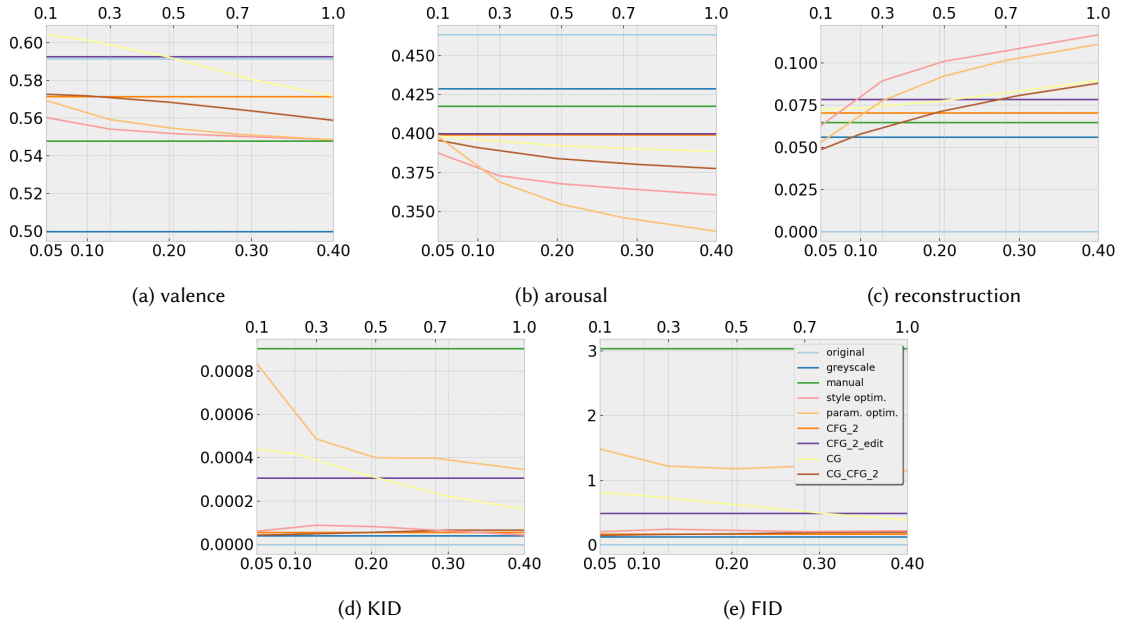


Fig. 5. Criteria alignment analysis: The plots show how the metrics evolve as the weighting of the objective terms that introduce emotional changes in the images increases. In each plot, the upper x-axis represents the values of w_2 for parametric optimization and style optimization, while the lower x-axis indicates the values of s for CG & CFG and CG.

For arousal, higher weights were consistently associated with reductions in arousal ($p < 0.03$). The terms for each approach were as follows: style optimization ($\beta_1 = -0.0274$, $p = 0.027$), parametric optimization ($\beta_1 = -0.0640$, $p = 0.017$), CG ($\beta_1 = -0.0282$, $p = 0.003$), and CG & CFG ($\beta_1 = -0.0513$, $p = 0.005$).

As anticipated, the reconstruction error (Fig. 5c) increased with the rising weight of the emotional adaptation objective, reflecting the greater modifications introduced to the original images. Despite these changes, the low KID (Fig. 5d) and FID scores (Fig. 5e) across baselines and weights confirm that the adapted images maintain high visual quality.

Qualitative findings. Figures 6 and 7 provide examples illustrating how the different approaches adjust images to achieve the desired effect. CG & CFG introduces changes not only to colors but also to the content, often resulting in plastic transformations. For example, in Figure 6f, the man appears older, and in Figure 7f, the tram also ages as the weighting of the adaptation objective increases. Similarly, CG modifies both the color and content of images, however, artifacts can appear (Figure 6g). NTO-instruct and NTO-edit produce comparable adjustments, but their lack of consistency is evident in both examples where they fail to adequately reduce valence and arousal to match the reference in both instances.

In contrast, style optimization and parametric optimization primarily alter the color values of images by introducing cooler tones (Figures 6i, 7h, 7i) or adding a red tint (Figure 6h). Similar changes are affected by manual (Figures 6c, 7c) Additional qualitative examples from this experiment are provided in Appendix C.

Analyzing changes in image properties. We also analyzed whether our approaches introduced changes to image properties in line with findings from previous research (Sec. 2.1). While these studies typically investigate how specific

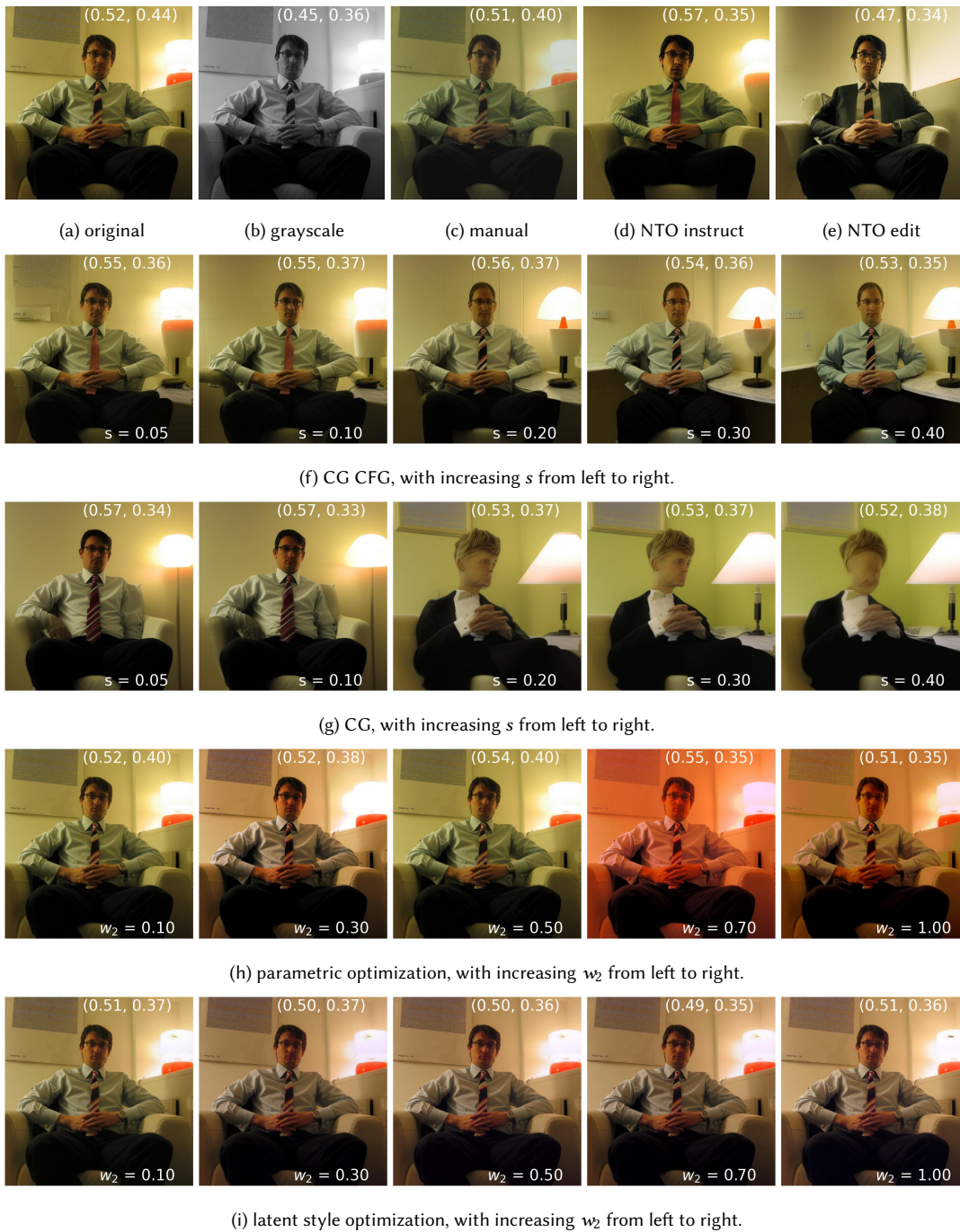


Fig. 6. Example result of COCO. Image caption: "A man in a shirt and tie sitting on a white chair next to a lamp."



Fig. 7. Example result of COCO. Image caption: "A trolley is going down the street while a car passes it."

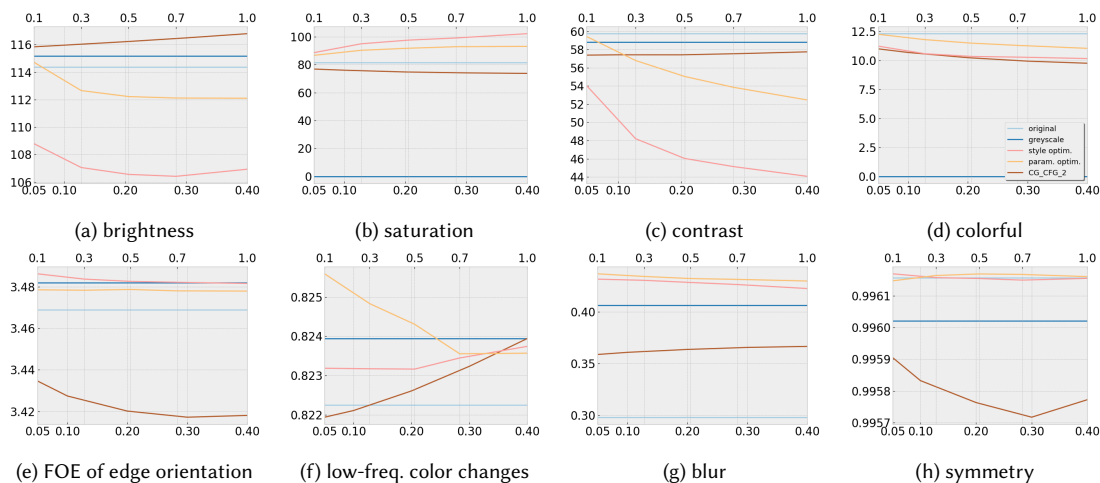


Fig. 8. Analyzing changes in image properties: The plots show how the metrics evolve as the weighting of the objective terms that introduce emotional changes in the images increases. In each plot, the upper x-axis represents the values of w_2 for parametric optimization and style optimization, while the lower x-axis indicates the values of s for CG & CFG.

image properties influence valence and arousal, our focus was on the inverse relationship. To this end, we hypothesized the expected effects of adaptation approaches on the respective image properties, based on the fact that these methods adjust images according to our defined *emotional reference*, and examined which of our proposed approaches (style optimization, parametric optimization, CG & CFG) support this hypothesis. We further compared them against the original set of images and the greyscale baseline.

Brightness is typically associated with positive valence [39, 105]. Given the slightly positive valence of the original images and our *emotional reference*, we expected a slight decrease in the brightness of adapted images. This expectation was not met by greyscale and CG & CFG. Conversely, style optimization and parametric optimization achieved the expected decrease in brightness.

Prior work links higher *saturation* levels to more positive valence and arousal [95, 103], suggesting that our approaches should reduce color saturation given the emotional reference. This expectation was true for the greyscale baseline. Similarly, CG & CFG decreased saturation, albeit to a lesser extent. Counterintuitively, style optimization and parametric optimization increased saturation.

Contrast is known to increase valence when enhanced and decrease it when reduced [111], suggesting that approaches should marginally reduce contrast given the slightly positive valence of the original images. This expectation was true for all approaches and greyscale.

Studies suggest that colored images enhance the positivity or negativity of valence and are slightly more arousing than greyscale images [7, 21]. Given our *emotional reference*, the colorfulness of adapted images should decrease. This was observed for all approaches.

A larger *1st-order entropy of edge orientations* coincides with higher arousal ratings [95]. As we minimized the arousal images elicit, we expected adapted images to possess a lower 1st-order entropy than the original images. This was true for CG & CFG but not for style optimization, parametric optimization, and greyscale.

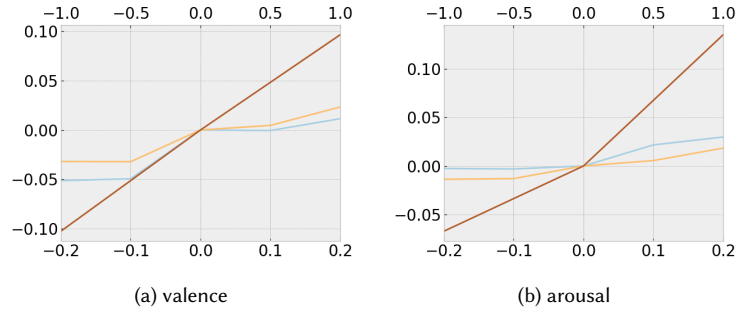


Fig. 9. Bidirectional emotional changes: The plots show how predicted valence and arousal evolve as the emotional reference of the algorithms is changed. In each plot, the lower x-axis represents the emotional reference for parametric optimization and style optimization, while the upper x-axis indicates the emotional reference for CG & CFG. The values at 0.0 represent the original image’s valence and arousal.

Images with predominantly *low-frequency changes in color and greyscale channels* tend to evoke higher arousal [34]. This means that images that are optimized for low-arousal should possess lower Z-score transformed wavelet coefficients than their unadjusted counterparts. This did not apply to any approach, as all exhibited greater low-frequency color changes than the original images, albeit with minor differences.

Introducing *blur* reduces both valence and arousal compared to their original counterparts [32], suggesting that our approaches should increase blur in the adapted images. This expectation was supported by the results of all approaches.

Symmetry is generally associated with positive valence and arousal [10–12, 15, 75]. Given our *emotional reference*, we expected adapted images to show lower levels of symmetry. This pattern was also evident in the CG & CFG and greyscale approaches, but not in style optimization and parametric optimization, although all differences are minor.

7.2 Bidirectional emotional changes

We conduct an additional experiment to determine whether CG & CFG, style optimization, and parametric optimization can optimize images for different reference points in the valence-arousal space.

For style optimization and parametric optimization, which primarily modify color values, initial experiments revealed that extreme emotional references often introduce artifacts (e.g., images becoming entirely black). Therefore, we define their reference points relative to the inferred valence and arousal values of each image. Specifically, we selected incremental adjustments of $[-0.2, -0.1, +0.1, +0.2]$ to both valence and arousal values as targets for optimization. In contrast, CG & CFG, capable of making more extensive plastic changes, can handle more extreme emotional references. Accordingly, we use the emotional references of valence = arousal = -1.0 and valence = arousal = 1.0 for this approach.

This experiment is conducted on a random subset of 500 images from the Instagram Influencer Dataset [58]. We use the same weights for the approaches as in the behavioral study (CG & CFG: $w = 2.0$, $s = 0.2$; style optimization: $w_1 = 1.0$, $w_2 = 0.2$; and parametric optimization: $w_1 = 1.0$, $w_2 = 0.2$).

7.2.1 Results. Figure 9 illustrates the emotional reference values plotted against the averaged inferred valence and arousal of all adapted images. The results indicate that the adaptation approaches achieve the intended directional emotional changes, albeit to a lesser degree than the reference values.

To formally evaluate this relationship, we fit an OLS model to the average valence and arousal values for style optimization and parametric optimization. For valence, the predictors for style optimization and parametric optimization

exhibit positive coefficients (0.1741 and 0.1470, respectively) and are statistically significant ($p < 0.03$), indicating a meaningful relationship. Similarly, for arousal, both approaches show positive coefficients (style optimization=0.0896, parametric optimization=0.0827) and significant results ($p < 0.03$), supporting a positive association between the emotional reference and the adapted outcomes. Note that the limited sample size impacts the generalizability of these findings. The small sample size of CG & CFG ($N = 3$) prevents fitting an OLS model to its results. Despite this, CG & CFG demonstrates a steeper positive slope for both valence and arousal compared to style optimization and parametric optimization, confirming with the expected positive relationships.



Fig. 10. Example result of bidirectional emotional change analysis. The emotional reference is displayed in the bottom-right corner, while the inferred valence and arousal values are shown in the top-right corner. Image caption: "A man and a woman standing closely with a historical building in the background."

Qualitative inspection of the results reveals distinct trends across the approaches. For style optimization and parametric optimization, an increase in the valence and arousal reference results in warmer colors in the adapted images, while more negative values typically yield cooler tones (subfigures b and c in Figures 10 & 11). In contrast, CG & CFG introduces plastic changes, such as making subjects appear more attractive and enhancing their smiles as the emotional reference increases (Figures 10). Additionally, CG & CFG produces images with greater detail and saturation as the emotional reference intensifies (Figure 11). Further qualitative results can be found in Appendix D.



Fig. 11. Example result of bidirectional emotional change analysis. The emotional reference is displayed in the bottom-right corner, while the inferred valence and arousal values are shown in the top-right corner. Image caption: "A serene, narrow street with cobblestones, a pink house with green shutters, and a multi-story building with ivy."

7.3 Adapting social media images

In this experiment, we assess the qualitative impact of our image adaptation approaches on social media images when adapted according to the defined *emotional reference*. Thus, we apply our methods to randomly sampled images from the Instagram Influencer Dataset [58].

7.3.1 Results. The qualitative results are shown in Figures 12 and 13. Across images, it is evident that style optimization and parametric optimization modify the low-level properties by introducing strong color hues (Figure 12a & d) or altering brightness, either lightening or darkening the image (Figure 13b & d). However, both approaches also produce samples with no noticeable changes (Figure 12b), or even enhance the image’s visual appeal (as seen with style optimization in Figure 12c and parametric optimization in Figure 13c).

In contrast to style optimization and parametric optimization, CG & CFG does not change the colorization of images. Instead, it introduces semantic changes to align images with the observed emotional reference patterns. Commonly observed changes include making subjects appear older (Figure 12a), less attractive (Figure 12b), adding layers of clothing (Figure 12c), or altering facial expressions (Figure 12d). Additionally, CG & CFG may remove subjects from images



(a) Subjects get older. Image caption: "A man in a dark suit and a woman in a dress posing together at a dining table."



(b) Subjects decline in attractiveness. Image caption: "Blonde woman dressed in black ripped jeans and black top posing outdoors."



(c) Subjects get clothed. Image caption: "The man is holding a cup and sitting shirtless on a bed with a scenic mountain view outside."



(d) Subjects' facial expression is changed. Image caption: "Woman practicing yoga in a modern kitchen."

Fig. 12. Social media images adapted using style optimization, original, parametric optimization, and CG & CFG (from left to right). Each image is representative for a type of change commonly induced through the CG & CFG diffusion algorithm (see sub-caption).



(a) Subjects get removed. Image caption: "Woman lying on a wooden deck above a calm water surface during a sunset."



(b) Subjects are reduced in size. Image caption: "Surfer riding a large ocean wave with people in the background."



(c) Animals appear less cute. Image caption: "A small dog sitting on a bed inside a camper van with mountains visible through the front window."



(d) Background becomes simpler. Image caption: "Person sitting under a tree gazing at the starry night sky with the Milky Way visible in the background."

Fig. 13. Social media images adapted using style optimization, original, parametric optimization, and CG & CFG (from left to right). Each image is representative for a type of change commonly induced through the CG & CFG diffusion algorithm (see sub-caption).

(Figure 13a), reduce their size (Figure 13b), make animals appear less cute (Figure 13c), or simplify the background (Figure 13d). Further qualitative results demonstrating these patterns can be found in Appendix E.

7.4 Discussion

Our analysis demonstrates that the proposed algorithms (CG & CFG, style optimization, parametric optimization), guided by a regressor, introduce image adaptations that align more closely with the *emotional reference* than other baseline approaches. For example, while manual effectively reduces valence, it fails to reduce arousal. CG succeeds in reducing both arousal and valence as per the *emotional reference*, though to a lesser extent than CG & CFG, style optimization, and parametric optimization. However, it introduces more artifacts into the images, as reflected in its higher KID and FID scores, greater reconstruction error, and qualitative results (Figure 6g). All approaches achieve KID and FID values indicative of high visual quality, but parametric optimization, CG, NTO-edit, and manual exhibit slightly weaker performance. These findings validate the effectiveness of regressor-guided adaptation for emotional property adjustments. Based on these results, we will prioritize CG & CFG, style optimization, and parametric optimization in subsequent user studies⁴.

Further evaluation of CG & CFG, style optimization, and parametric optimization examines whether their image property changes align with prior research and the *emotional reference*. The approaches align with expectations for *contrast*, *colorfulness*, and *blur*. For other properties (*brightness*, *saturation*, *1st-order entropy of edge orientations*) the fulfillment of the hypothesized outcomes varies, with some approaches aligning with expectations and others diverging. Properties such as *low-frequency color changes* and *symmetry* exhibit only minimal differences from the original images across all approaches.

All proposed approaches could also introduce meaningful changes given different emotional references. A statistical analysis reveals positive associations between the emotional references and adapted outcomes for style optimization and parametric optimization. While results of CG & CFG could not be modeled due to a limited sample size, it shows even stronger directional changes than the other two approaches. The fact that the results demonstrate the intended directional emotional changes to a lesser extent than the reference values indicates that our dual-objective optimization can balance emotional modulation with preserving the alignment to the original images. Qualitative inspection highlights distinctive trends: style optimization and parametric optimization tend to modify colors (warmer tones for higher valence/arousal and cooler tones for lower values), whereas CG & CFG introduces plastic changes, such as enhancing smiles and attractiveness as valence and arousal increase.

Qualitative analysis of the social media images adapted by our approaches reveals patterns of change with which the emotional properties of the images were shifted toward the desired *emotional reference*. style optimization and parametric optimization primarily alter low-level image properties, such as color hues and brightness, but sometimes result in images with no noticeable changes or even improvements in visual appeal. In contrast, CG & CFG does not modify colorization, instead introducing semantic changes to align images with emotional reference patterns, such as making subjects appear older or less attractive, altering facial expressions, or adding clothing.

In summary, our proposed approaches successfully modify image properties to achieve the desired emotional changes (better than baselines), even though not all hypothesized properties are consistently addressed, and some remain unchanged. Notably, CG & CFG introduces perceptual changes beyond emotional adjustments, such as increasing the apparent age of a subject. However, all three approaches also yield results that are either counterintuitive given the

⁴We reduce approaches to keep user studies within a reasonable time frame.

optimization target (as seen with style optimization and parametric optimization) or, in the case of CG & CFG, generate artifacts, particularly around the extremities of human subjects.

8 BEHAVIORAL STUDY

The study evaluates the developed computational image adaptation methods in their effectiveness in reducing emotional arousal and neutralizing valence in viewers of images while keeping a high image quality (RQ1).

8.1 Study design

In the following, we detail conditions, stimuli, task and participants of the experiment.

Stimuli. The stimuli we used in this study stem from the Nencki Affective Picture System (NAPS) [76]. It consists of 1,356 realistic, high-quality photographs for which affective ratings were collected from 204 participants. They are divided into five categories: people, faces, animals, objects, and landscapes. We selected images from the categories of people, faces, animals, and landscapes as they represent genres frequently seen on social media [63].

Following the approach of [83], we divided the valence-arousal space into distinct regions. We excluded regions that are positioned near the optimization target (low arousal/neutral valence) as for images in these regions the adaptations are minimal by design. The final image selection was drawn from four clusters: mid arousal/low valence, high arousal/low valence, mid arousal/high valence, and high arousal/high valence (see Figure 14). For the task, we selected 17 images from these clusters that appeared to induce strong emotions in viewers. To keep the study within a certain time frame and to have an equal number of images selected per cluster, we selected a subset of 12 images (three per cluster). Thus, we excluded 5 images where changes introduced by algorithms were barely visible or introduced artifacts. In addition, we sampled 5 images from the whole valence arousal spectrum to show in the calibration phase of the experiment. As the usage rights of NAPS prohibit publishing its images, the stimuli are not displayed here.

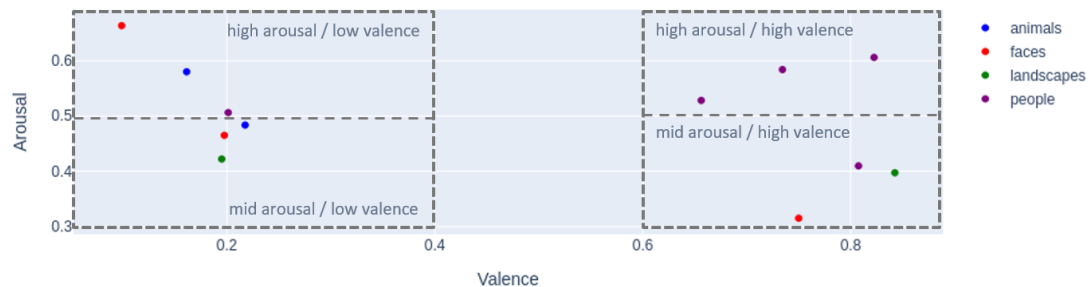


Fig. 14. Location of selected stimuli within the valence arousal space of the Circumplex Model of Affect [98]. To select images from a spectrum of valence and arousal values, they were drawn from four clusters: mid arousal/low valence, high arousal/low valence, high arousal/high valence, and mid arousal/high valence.

The 12 images form a block that was adapted according to each adaptation condition. For the order within each block, we followed the study design of [83], starting and ending with lower-arousal, positive images to ease participants into the new technique and leave them with a positive sentiment. Specifically, we began and concluded each block with images from the mid arousal/high valence cluster, then proceeded counterclockwise through the specified clusters in the valence-arousal space.

Task. Participants were asked to observe an emotional image for a minimum of five seconds. After these five seconds, participants could choose to either continue viewing the image or proceed with the experiment by pressing the space key on their keyboard. Following that, participants were directed to the next webpage, where they were asked to complete a validated questionnaire, which collects emotional valence and arousal ratings [16]. Additionally, they were asked to rate a Likert item assessing the quality of the image (adjusted from [83]). To prevent emotional contamination between images, we showed a neutral stimulus after each image-questionnaire pair.

Conditions. The study conditions included three of our three proposed computational approaches, along with the images in their original form and after applying a greyscale filter. Based on the results of our technical evaluation and additional empirical tests, we selected the adaptation weights to balance the trade-off between reducing evoked emotions and maintaining fidelity to the original images. The weights for each approach were CG & CFG: $w = 2.0$, $s = 0.2$; style optimization: $w_1 = 1.0$, $w_2 = 0.2$; parametric optimization: $w_1 = 1.0$, $w_2 = 0.15$.

Taking inspiration from similar work [13, 83], the study was conducted as within-subjects design with one factor (IMAGE ADAPTATION TECHNIQUE) and five levels (*original, grayscale, diffusion, style opt., param. opt.*). With each adaptation approach, we adapted the block of images. Each block with a fixed order of images was presented to participant in each condition. To avoid order effects, we used latin-square counterbalancing to adjust the order of conditions between participants. Nonetheless, we tracked the order of blocks as shown to participants to be able to recognize potential order biases. To monitor fatigue effects, we noted at which trial a picture was presented.

Procedure. Participants recruited via a crowdsourcing platform began by signing a consent form and completing pre-questionnaires on our experimental platform. They then viewed a brief study introduction and familiarized themselves with the setup using a trial run featuring a placeholder image. Following a two-minute relaxation video, participants received on-screen instructions to start the experiment.

The experiment involved sequential exposure to calibration images followed by five blocks of images per condition (see Stimuli for details), with self-assessments after each image. Upon completion, participants received a code to claim a monetary reward of 4.5 GBP. The study took approximately 30 minutes per participant.

Participants. We conducted an a priori power analysis to establish the minimum sample size needed to test our hypotheses. Based on Cohen's f effect sizes observed in similar studies (0.25–1.5; [7, 32]), we adopted a conservative effect size of 0.2. To achieve 95% power with $\alpha = 0.05$ for a repeated-measures ANOVA with five conditions, we calculated a required sample size of $N = 48$. Consequently, we recruited 59 participants (33 female, 26 male), ages 18–74 ($M=36$, $SD=11.5$) from an online crowd-sourcing platform. We excluded three participants whose data clearly indicated they did not perform the task faithfully (i.e., they rated all images identically). The data of the remaining 56 participants was used in the analysis. Importantly, the significance of the results remains unchanged regardless of whether these outliers are included or excluded.

8.2 Results

In the following, we present the results of the behavioral study. For significance testing, we conducted an ANOVA with sphericity corrections applied to all within-subject factors. Notably, the significance of the results remain consistent regardless of whether the sphericity correction is applied. Pairwise comparisons were performed using t-tests to evaluate whether the results aligned with the hypotheses outlined in the study's pre-registration [41]. Specifically, these

hypotheses focus on the impact of adaptation algorithms on subjective ratings, compared to the effects of both colored original images and their grayscale counterparts. Figure 15 shows overview of the results of the study.

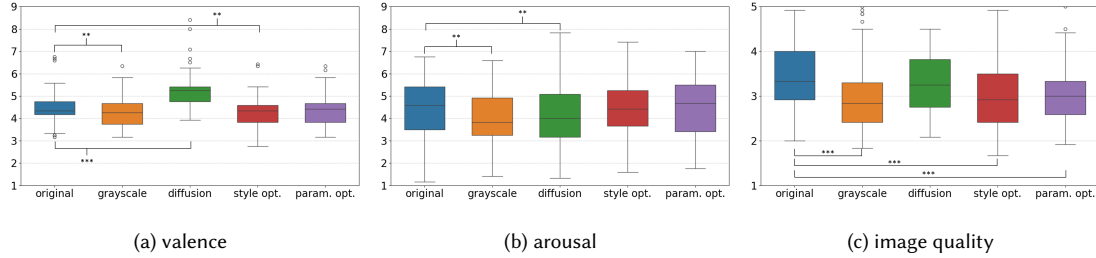


Fig. 15. Results of calibration study: Boxplots of subjective ratings of participants for valence (a), arousal (b), and image quality (c). Only significant differences compared to the original images are indicated (* $p < 0.05$, ** $p < 0.01$, and *** $p < 0.001$)

We found a significant effect of IMAGE ADAPTATION TECHNIQUE on valence ratings [$F_{2,80,153.84} = 69.32$, $p < .001$, $\eta_p^2 = .56$]. Post-hoc tests have shown that *diffusion* caused an increase in valence ratings over *original* as well as *grayscale* ($p < .0001$ for both). Conversely, *style opt.* and *grayscale* caused a decrease in valence ratings over *original* ($p < .003$ for both). No significant differences were observed between other conditions in comparison with *original* and *grayscale*.

The ANOVA also showed that there was a significant effect of the IMAGE ADAPTATION TECHNIQUE on arousal ratings [$F_{3,24,178.08} = 7.79$, $p < .001$, $\eta_p^2 = .12$]. Post-hoc tests have shown that *diffusion* and *grayscale* both caused lower arousal ratings than default ($p < .002$). They also revealed *grayscale* caused lower arousal ratings than both *style opt.*, *param. opt.* ($p < .001$). Our analysis did not find an effect in other comparisons.

The ANOVA further revealed a main effect of IMAGE ADAPTATION TECHNIQUE on image quality [$F_{2,73,150.19} = 10.04$, $p < .001$, $\eta_p^2 = .15$]. Pairwise comparisons have shown that *grayscale*, *param. opt.*, and *style opt.* caused lower image quality ratings than *original* (all $p < .0001$). Conversely, *diffusion* exhibited higher image quality ratings than *grayscale* ($p = .02$). No other effects were found.

No significant differences were found in the case of observation durations.

8.3 Discussion

Our experiment examined whether the changes introduced to images by our adaptation algorithms effectively altered the perceived emotions of viewers. While this was not observed for *param. opt.* and *style opt.*, the *diffusion* condition led to higher valence ratings than all other conditions, with a mean (5.23) closer to the *emotional reference* (expected to be 5 when transformed to the Likert scale) compared to other conditions (*original*: 4.43; *grayscale*: 4.23; *param. opt.*: 4.32; *style opt.*: 4.23). Additionally, *diffusion* elicited lower arousal ratings than *original*, *param. opt.*, and *style opt.*, while not differing significantly from *grayscale*.

Importantly, *diffusion* was the only condition that maintained perceived image quality comparable to *original*. This highlights its potential to introduce emotional changes while preserving the overall integrity of the image.

9 CONCLUSION & FUTURE WORK

In this work, we have shown that a diffusion-based approach using classifier guidance in combination with classifier-free guidance can introduce image edits that regulate the emotional response of viewers. While the approach can also

change the colorization of images, it achieves the emotional shift primarily through semantic content changes such as adding additional layers of clothing, simplifying the background, or aging the appearance of subjects.

In future work, we will investigate the impact of these image adaptations on internet user behavior. Specifically, we aim to determine whether emotionally altered images can reduce the time users spend browsing a social media feed (RQ2). In addition, we examine whether these adapted images can mitigate the tendency for negative social comparisons. Social media often emphasizes aspirational aspects of life, such as luxury, beauty, and happiness, which can create a stark contrast to users' everyday experiences. We hypothesize that more neutral and less arousing images will reduce these contrasts, potentially leading to fewer feelings of inadequacy.

REFERENCES

- [1] Itzhak Aharon, Nancy Etcoff, Dan Ariely, Christopher F Chabris, Ethan O'connor, and Hans C Breiter. 2001. Beautiful faces have variable reward value: fMRI and behavioral evidence. *Neuron* 32, 3 (2001), 537–551.
- [2] Hosam Al-Samarraie, Kirfi-Aliyu Bello, Ahmed Ibrahim Alzahrani, Andrew Paul Smith, and Chikezie Emele. 2021. Young users' social media addiction: causes, consequences and preventions. *Information Technology & People* (2021). <https://doi.org/10.1108/itp-11-2020-0753>
- [3] Afsheen Rafaqat Ali and Mohsen Ali. 2017. Automatic image transformation for inducing affect. *arXiv preprint arXiv:1707.08148* (2017).
- [4] Jie An, Tianlang Chen, Songyang Zhang, and Jiebo Luo. 2021. Global Image Sentiment Transfer. In *2020 25th International Conference on Pattern Recognition (ICPR)*. IEEE, 6267–6274.
- [5] Cecilie Schou Andreassen. 2015. Online social network site addiction: A comprehensive review. *Current Addiction Reports* 2, 2 (2015), 175–184.
- [6] Apple. 2023. Keep track of your screen time on iPhone. apple.com (Accessed: 11.01.2023).
- [7] Valeria Bekhtereva and Matthias M Müller. 2017. Bringing color to emotion: The influence of color on attentional bias to briefly presented emotional images. *Cognitive, Affective, & Behavioral Neuroscience* 17, 5 (2017), 1028–1047.
- [8] Jonah Berger and Katherine L Milkman. 2012. What makes online content viral? *Journal of marketing research* 49, 2 (2012), 192–205.
- [9] D.E. Berlyne. 1971. *Aesthetics and Psychobiology*. Appleton-Century-Crofts. <https://books.google.ch/books?id=o5TWAAAAMAAJ>
- [10] Marco Bertamini, Alexis Makin, and Giulia Rampone. 2013. Implicit association of symmetry with positive valence, high arousal and simplicity. *i-Perception* 4, 5 (2013), 317–327.
- [11] Marco Bertamini, Giulia Rampone, Alexis DJ Makin, and Andrew Jessop. 2019. Symmetry preference in shapes, faces, flowers and landscapes. *PeerJ* 7 (2019), e7078.
- [12] Marco Bertamini, Juha Silvanto, Anthony M Norcia, Alexis DJ Makin, and Johan Wagemans. 2018. The neural basis of visual symmetry and its role in mid-and high-level visual processing. *Annals of the New York Academy of Sciences* 1426, 1 (2018), 111–126.
- [13] Lonni Besançon, Amir Semmo, David Biau, Bruno Frachet, Virginie Pineau, El Hadi Sariali, Rabah Taouachi, Tobias Isenberg, and Pierre Dragicevic. 2018. Reducing affective responses to surgical images through color manipulation and stylization. In *Expressive*. 11–1.
- [14] Anselm Brachmann and Christoph Redies. 2016. Using convolutional neural network filters to measure left-right mirror symmetry in images. *Symmetry* 8, 12 (2016), 144.
- [15] Anselm Brachmann and Christoph Redies. 2017. Computational and experimental approaches to visual aesthetics. *Frontiers in computational neuroscience* 11 (2017), 102.
- [16] Margaret M Bradley and Peter J Lang. 1994. Measuring emotion: the self-assessment manikin and the semantic differential. *Journal of behavior therapy and experimental psychiatry* 25, 1 (1994), 49–59.
- [17] William J. Brady, Julian A. Wills, John T. Jost, Joshua A. Tucker, and Jay J. Van Bavel. 2017. Emotion shapes the diffusion of moralized content in social networks. *Proceedings of the National Academy of Sciences* 114, 28 (2017), 7313–7318. <https://doi.org/10.1073/pnas.1618923114>
- [18] Sharon Brehm and Jack Brehm. 2013. *Psychological reactance: A theory of freedom and control*. Academic Press.
- [19] Tim Brooks, Aleksander Holynski, and Alexei A Efros. 2023. Instructpix2pix: Learning to follow image editing instructions. In *Proceedings of the IEEE/CVF Conference on Computer Vision and Pattern Recognition*. 18392–18402.
- [20] Moira Burke and Robert E. Kraut. 2016. The Relationship Between Facebook Use and Well-Being Depends on Communication Type and Tie Strength. *Journal of Computer-Mediated Communication* 21, 4 (05 2016), 265–281. <https://doi.org/10.1111/jcc4.12162> arXiv:<https://academic.oup.com/jcmc/article-pdf/21/4/265/22316334/jcmc.com0265.pdf>
- [21] Maya E Cano, Quetzal A Class, and John Polich. 2009. Affective valence, stimulus attributes, and P300: color vs. black/white and normal vs. scrambled images. *International Journal of Psychophysiology* 71, 1 (2009), 17–24.
- [22] Luis Carretié, Manuel Tapia, Sara López-Martín, and Jacobo Albert. 2019. EmoMadrid: An emotional pictures database for affect research. *Motivation and Emotion* 43 (2019), 929–939.
- [23] Tianlang Chen, Wei Xiong, Haitian Zheng, and Jiebo Luo. 2020. Image sentiment transfer. In *Proceedings of the 28th ACM International Conference on Multimedia*. 4407–4415.

- [24] Yunjey Choi, Minje Choi, Munyoung Kim, Jung-Woo Ha, Sunghun Kim, and Jaegul Choo. 2018. Stargan: Unified generative adversarial networks for multi-domain image-to-image translation. In *Proceedings of the IEEE conference on computer vision and pattern recognition*. 8789–8797.
- [25] Yunjey Choi, Youngjung Uh, Jaejun Yoo, and Jung-Woo Ha. 2020. Stargan v2: Diverse image synthesis for multiple domains. In *Proceedings of the IEEE/CVF conference on computer vision and pattern recognition*. 8188–8197.
- [26] covenanteyes.com. 2022. CovenantEyes. covenanteyes.com (Accessed: 08.07.2022).
- [27] Frederique Crete, Thierry Dolmieri, Patricia Ladret, and Marina Nicolas. 2007. The blur effect: perception and estimation with a new no-reference perceptual blur metric. In *Human vision and electronic imaging XII*, Vol. 6492. SPIE, 196–206.
- [28] Claudia Damiano, Dirk B Walther, and William A Cunningham. 2021. Cues to Danger: Contour Features Predict Valence and Threat Judgements in Scenes. (2021).
- [29] Elise S Dan-Glauser and Klaus R Scherer. 2011. The Geneva affective picture database (GAPED): a new 730-picture database focusing on valence and normative significance. *Behavior research methods* 43 (2011), 468–477.
- [30] Stefano d’Apolito, Danda Pani Paudel, Zhiwu Huang, Andrés Romero, and Luc Van Gool. 2021. Ganmut: Learning interpretable conditional space for gamut of emotions. In *Proceedings of the IEEE/CVF Conference on Computer Vision and Pattern Recognition*. 568–577.
- [31] DataReportal, & We Are Social, & Meltwater. 2023. Most popular websites worldwide as of November 2022, by total visits. <https://www.statista.com/statistics/1201880/most-visited-websites-worldwide/>
- [32] Andrea De Cesarei and Maurizio Codispoti. 2010. Effects of picture size reduction and blurring on emotional engagement. *PLoS One* 5, 10 (2010), e13399.
- [33] Dian A. de Vries, A. Marthe Möller, Marieke S. Wieringa, Anniek W. Eigenraam, and Kirsten Hamelink. 2018. Social Comparison as the Thief of Joy: Emotional Consequences of Viewing Strangers’ Instagram Posts. *Media Psychology* 21, 2 (April 2018), 222–245. <https://doi.org/10.1080/15213269.2016.1267647>
- [34] Sylvain Delplanque, Karim N’diaye, Klaus Scherer, and Didier Grandjean. 2007. Spatial frequencies or emotional effects?: A systematic measure of spatial frequencies for IAPS pictures by a discrete wavelet analysis. *Journal of neuroscience methods* 165, 1 (2007), 144–150.
- [35] Prafulla Dhariwal and Alexander Nichol. 2021. Diffusion models beat gans on image synthesis. *Advances in Neural Information Processing Systems* 34 (2021), 8780–8794.
- [36] Nir Diamant, Dean Zadok, Chaim Baskin, Eli Schwartz, and Alex M Bronstein. 2019. Beholder-GAN: Generation and beautification of facial images with conditioning on their beauty level. In *2019 IEEE International Conference on Image Processing (ICIP)*. IEEE, 739–743.
- [37] forestapp.cc. 2018. Forest - Stay focused, be present. forestapp.cc (Accessed: 02.01.2023).
- [38] freedom.to. 2022. Freedom to be incredibly productive. freedom.to (Accessed: 08.07.2022).
- [39] Xiao-Ping Gao, John H Xin, Tetsuya Sato, Aran Hansuebsai, Marcello Scalzo, Kanji Kajiwara, Shing-Sheng Guan, Josep Valldeperas, Manuel José Lis, and Monica Billger. 2007. Analysis of cross-cultural color emotion. *Color Research & Application: Endorsed by Inter-Society Color Council, The Colour Group (Great Britain), Canadian Society for Color, Color Science Association of Japan, Dutch Society for the Study of Color, The Swedish Colour Centre Foundation, Colour Society of Australia, Centre Français de la Couleur* 32, 3 (2007), 223–229.
- [40] David Garcia, Arvid Kappas, Dennis Küster, and Frank Schweitzer. 2016. The dynamics of emotions in online interaction. *Royal Society open science* 3, 8 (2016), 160059.
- [41] Christoph Gebhardt, Robin Willardt, and Christian Holz. 2024. Pre-registration for "Effect of image adaptations on passive social media use". *OSF* (2024). <https://doi.org/10.17605/OSF.IO/52VYF>
- [42] Gernot Gerger, Helmut Leder, Pablo PL Tinio, and Annkathrin Schacht. 2011. Faces versus patterns: Exploring aesthetic reactions using facial EMG. *Psychology of Aesthetics, Creativity, and the Arts* 5, 3 (2011), 241.
- [43] getcoldturkey.com. 2022. Cold Turkey - Your future self will thank you. getcoldturkey.com (Accessed: 08.07.2022).
- [44] Lore Goetschalckx, Alex Andonian, Aude Oliva, and Phillip Isola. 2019. Ganalyze: Toward visual definitions of cognitive image properties. In *Proceedings of the IEEE/CVF International Conference on Computer Vision*. 5744–5753.
- [45] Adam M Goodman, Jeffrey S Katz, and Michael N Dretsch. 2016. Military Affective Picture System (MAPS): A new emotion-based stimuli set for assessing emotional processing in military populations. *Journal of behavior therapy and experimental psychiatry* 50 (2016), 152–161.
- [46] Natasha Gupta and Julia D. Irwin. 2016. In-class distractions: The role of Facebook and the primary learning task. *Computers in Human Behavior* 55 (2016), 1165–1178. <https://doi.org/10.1016/j.chb.2014.10.022>
- [47] Anke Haberkamp, Julia Anna Glombiewski, Philipp Schmidt, and Antonia Barke. 2017. The Disgust-Related-Images (DIRTI) database: Validation of a novel standardized set of disgust pictures. *Behaviour research and therapy* 89 (2017), 86–94.
- [48] Amanda C Hahn and David I Perrett. 2014. Neural and behavioral responses to attractiveness in adult and infant faces. *Neuroscience & Biobehavioral Reviews* 46 (2014), 591–603.
- [49] David Hasler and Sabine E Suesstrunk. 2003. Measuring colorfulness in natural images. In *Human vision and electronic imaging VIII*, Vol. 5007. SPIE, 87–95.
- [50] Jonathan Ho, Ajay Jain, and Pieter Abbeel. 2020. Denoising diffusion probabilistic models. *Advances in Neural Information Processing Systems* 33 (2020), 6840–6851.
- [51] Jonathan Ho and Tim Salimans. 2022. Classifier-free diffusion guidance. *arXiv preprint arXiv:2207.12598* (2022).
- [52] Yuanming Hu, Hao He, Chenxi Xu, Baoyuan Wang, and Stephen Lin. 2018. Exposure: A white-box photo post-processing framework. *ACM Transactions on Graphics (TOG)* 37, 2 (2018), 1–17.

- [53] Xun Huang, Ming-Yu Liu, Serge Belongie, and Jan Kautz. 2018. Multimodal unsupervised image-to-image translation. In *Proceedings of the European conference on computer vision (ECCV)*. 172–189.
- [54] Katherine Humphrey, Geoffrey Underwood, and Tony Lambert. 2012. Saliency of the lambs: A test of the saliency map hypothesis with pictures of emotive objects. *Journal of Vision* 12, 1 (2012), 22–22.
- [55] JDev. 2019. News Feed Eradicator. <chrome.google.com/nfe> (Accessed: 02.01.2023).
- [56] Hye-Rin Kim, Yeong-Seok Kim, Seon Joo Kim, and In-Kwon Lee. 2018. Building emotional machines: Recognizing image emotions through deep neural networks. *IEEE Transactions on Multimedia* 20, 11 (2018), 2980–2992.
- [57] Jaejeung Kim, Hayoung Jung, Minsam Ko, and Uichin Lee. 2019. GoalKeeper: exploring interaction lockout mechanisms for regulating smartphone use. *Proceedings of the ACM on Interactive, Mobile, Wearable and Ubiquitous Technologies* 3, 1 (2019), 1–29.
- [58] Seungbae Kim, Jyun-Yu Jiang, Masaki Nakada, Jinyoung Han, and Wei Wang. 2020. Multimodal Post Attentive Profiling for Influencer Marketing. In *Proceedings of The Web Conference 2020*. 2878–2884.
- [59] Minsam Ko, Subin Yang, Joonwon Lee, Christian Heizmann, Jinyoung Jeong, Uichin Lee, Daehee Shin, Koji Yatani, Junehwa Song, and Kyong-Mee Chung. 2015. NUGU: a group-based intervention app for improving self-regulation of limiting smartphone use. In *Proceedings of the 18th ACM conference on computer supported cooperative work & social computing*. 1235–1245.
- [60] Geza Kovacs, Zhengxuan Wu, and Michael S Bernstein. 2018. Rotating online behavior change interventions increases effectiveness but also increases attrition. *Proceedings of the ACM on HCI 2, CSCW* (2018).
- [61] Benedek Kurdi, Shayn Lozano, and Mahzarin R Banaji. 2017. Introducing the open affective standardized image set (OASIS). *Behavior research methods* 49 (2017), 457–470.
- [62] Peter J Lang, Margaret M Bradley, Bruce N Cuthbert, et al. 1997. International affective picture system (IAPS): Technical manual and affective ratings. *NIMH Center for the Study of Emotion and Attention* 1, 39-58 (1997), 3.
- [63] Helmut Leder, Jussi Hakala, Veli-Tapani Peltoketo, Christian Valuch, and Matthew Pelowski. 2022. Swipes and Saves: A Taxonomy of Factors Influencing Aesthetic Assessments and Perceived Beauty of Mobile Phone Photographs. *Frontiers in Psychology* 13 (2022), 786977–786977.
- [64] Hsin-Ying Lee, Hung-Yu Tseng, Jia-Bin Huang, Maneesh Singh, and Ming-Hsuan Yang. 2018. Diverse image-to-image translation via disentangled representations. In *Proceedings of the European conference on computer vision (ECCV)*. 35–51.
- [65] Liu Yi Lin, Jaime E Sidani, Ariel Shensa, Ana Radovic, Elizabeth Miller, Jason B Colditz, Beth L Hoffman, Leila M Giles, and Brian A Primack. 2016. Association between social media use and depression among US young adults. *Depression and anxiety* 33, 4 (2016), 323–331.
- [66] Tsung-Yi Lin, Michael Maire, Serge Belongie, James Hays, Pietro Perona, Deva Ramanan, Piotr Dollár, and C Lawrence Zitnick. 2014. Microsoft coco: Common objects in context. In *Computer Vision—ECCV 2014: 13th European Conference, Zurich, Switzerland, September 6–12, 2014, Proceedings, Part V 13*. Springer, 740–755.
- [67] Danielle Lottridge, Eli Marschner, Ellen Wang, Maria Romanovsky, and Clifford Nass. 2012. Browser design impacts multitasking. In *Proceedings of the human factors and Ergonomics Society Annual Meeting*, Vol. 56. SAGE Publications Sage CA: Los Angeles, CA, 1957–1961.
- [68] Todd Love, Christian Laier, Matthias Brand, Linda Hatch, and Raju Hajela. 2015. Neuroscience of internet pornography addiction: A review and update. *Behavioral sciences* 5, 3 (2015), 388–433.
- [69] Cheng Lu, Yuhao Zhou, Fan Bao, Jianfei Chen, Chongxuan Li, and Jun Zhu. 2022. Dpm-solver++: Fast solver for guided sampling of diffusion probabilistic models. *arXiv preprint arXiv:2211.01095* (2022).
- [70] Tao Lu, Hongxiao Zheng, Tianying Zhang, Xuhai “Orson” Xu, and Anhong Guo. 2024. InteractOut: Leveraging Interaction Proxies as Input Manipulation Strategies for Reducing Smartphone Overuse. In *Proceedings of the CHI Conference on Human Factors in Computing Systems*. 1–19.
- [71] Kai Lukoff, Ulrik Lyngs, and Lize Alberts. 2022. Designing to support autonomy and reduce psychological reactance in digital self-control tools. In *Position Papers for the Workshop “Self-Determination Theory in HCI: Shaping a Research Agenda” at the Conference on Human Factors in Computing Systems (CHI’22)*, Vol. 5.
- [72] Ulrik Lyngs, Kai Lukoff, Laura Csuka, Petr Slovák, Max Van Kleek, and Nigel Shadbolt. 2022. The Goldilocks level of support: Using user reviews, ratings, and installation numbers to investigate digital self-control tools. *International journal of human-computer studies* 166 (2022), 102869.
- [73] Ulrik Lyngs, Kai Lukoff, Petr Slovak, Reuben Binns, Adam Slack, Michael Inzlicht, Max Van Kleek, and Nigel Shadbolt. 2019. Self-control in cyberspace: Applying dual systems theory to a review of digital self-control tools. In *proceedings of the 2019 CHI conference on human factors in computing systems*. 1–18.
- [74] Ulrik Lyngs, Kai Lukoff, Petr Slovak, William Seymour, Helena Webb, Marina Jirotko, Jun Zhao, Max Van Kleek, and Nigel Shadbolt. 2020. ‘I Just Want to Hack Myself to Not Get Distracted’: Evaluating Design Interventions for Self-Control on Facebook. In *Proceedings of the 2020 CHI Conference on Human Factors in Computing Systems* (Honolulu, HI, USA) (CHI ’20). ACM, New York, NY, USA, 15 pages. <https://doi.org/10.1145/3313831.3376672>
- [75] Alexis DJ Makin, Moon M Wilton, Anna Pecchinenda, and Marco Bertamini. 2012. Symmetry perception and affective responses: A combined EEG/EMG study. *Neuropsychologia* 50, 14 (2012), 3250–3261.
- [76] Artur Marchewka, Łukasz Żurawski, Katarzyna Jednoróg, and Anna Grabowska. 2014. The Nencki Affective Picture System (NAPS): Introduction to a novel, standardized, wide-range, high-quality, realistic picture database. *Behavior research methods* 46 (2014), 596–610.
- [77] Maurizio Mauri, Pietro Cipresso, Anna Balgera, Marco Villamira, and Giuseppe Riva. 2011. Why Is Facebook So Successful? Psychophysiological Measures Describe a Core Flow State While Using Facebook. *Cyberpsychology, Behavior, and Social Networking* 14, 12 (Dec. 2011), 723–731. <https://doi.org/10.1089/cyber.2010.0377>

- [78] Youssef A Mejjati, Celso F Gomez, Kwang In Kim, Eli Shechtman, and Zoya Bylinskii. 2020. Look here! a parametric learning based approach to redirect visual attention. In *European Conference on Computer Vision*. Springer, 343–361.
- [79] Laura Miccoli, Rafael Delgado, Pedro Guerra, Francesco Versace, Sonia Rodriguez-Ruiz, and M Carmen Fernández-Santaella. 2016. Affective pictures and the Open Library of Affective Foods (OLAF): tools to investigate emotions toward food in adults. *PLoS one* 11, 8 (2016), e0158991.
- [80] Aswin Mohan. 2019. LessPhone. play.google.com/apps/lessphone (Accessed: 02.01.2023).
- [81] Ron Mokady, Amir Hertz, Kfir Aberman, Yael Pritch, and Daniel Cohen-Or. 2023. Null-text inversion for editing real images using guided diffusion models. In *Proceedings of the IEEE/CVF Conference on Computer Vision and Pattern Recognition*. 6038–6047.
- [82] Alberto Monge Roffarello and Luigi De Russis. 2019. The race towards digital wellbeing: Issues and opportunities. In *Proceedings of the 2019 CHI conference on human factors in computing systems*. 1–14.
- [83] David Mould, Regan L Mandryk, and Hua Li. 2012. Emotional response and visual attention to non-photorealistic images. *Computers & Graphics* 36, 6 (2012), 658–672.
- [84] Karen Nelson-Field, Erica Riebe, and Kellie Newstead. 2013. The Emotions that Drive Viral Video. *Australasian Marketing Journal* 21, 4 (2013), 205–211. <https://doi.org/10.1016/j.ausmj.2013.07.003>
- [85] Lauri Nummenmaa, Jari K Hietanen, Pekka Santtila, and Jukka Hyönä. 2012. Gender and visibility of sexual cues influence eye movements while viewing faces and bodies. *Archives of sexual behavior* 41, 6 (2012), 1439–1451.
- [86] Chanjong Park and In-Kwon Lee. 2020. Emotional landscape image generation using generative adversarial networks. In *Proceedings of the Asian Conference on Computer Vision*.
- [87] Eli Peli. 1990. Contrast in complex images. *JOSA A* 7, 10 (1990), 2032–2040.
- [88] Kuan-Chuan Peng, Tsuhan Chen, Amir Sadovnik, and Andrew C Gallagher. 2015. A mixed bag of emotions: Model, predict, and transfer emotion distributions. In *Proceedings of the IEEE conference on computer vision and pattern recognition*. 860–868.
- [89] Joanna Pilarczyk and Michał Kuniecki. 2014. Emotional content of an image attracts attention more than visually salient features in various signal-to-noise ratio conditions. *Journal of Vision* 14, 12 (2014), 4–4.
- [90] Charlie Pinder, Jose Ignacio Rocca, Benjamin R Cowan, and Russell Beale. 2019. Push away the smartphone: Investigating methods to counter problematic smartphone use. In *Extended Abstracts of the 2019 CHI Conference on Human Factors in Computing Systems*.
- [91] Dustin Podell, Zion English, Kyle Lacey, Andreas Blattmann, Tim Dockhorn, Jonas Müller, Joe Penna, and Robin Rombach. 2023. Sdxl: Improving latent diffusion models for high-resolution image synthesis. *arXiv preprint arXiv:2307.01952* (2023).
- [92] qustodio.com. 2022. Qustudio - parental control and digital wellbeing. qustodio.com (Accessed: 08.07.2022).
- [93] Alec Radford, Jong Wook Kim, Chris Hallacy, Aditya Ramesh, Gabriel Goh, Sandhini Agarwal, Girish Sastry, Amanda Askell, Pamela Mishkin, Jack Clark, et al. 2021. Learning transferable visual models from natural language supervision. In *International conference on machine learning*. PMLR, 8748–8763.
- [94] Christoph Redies, Anselm Brachmann, and Johan Wagemans. 2017. High entropy of edge orientations characterizes visual artworks from diverse cultural backgrounds. *Vision Research* 133 (2017), 130–144.
- [95] Christoph Redies, Maria Grebenkina, Mahdi Mohseni, Ali Kaduhm, and Christian Dobel. 2020. Global image properties predict ratings of affective pictures. *Frontiers in psychology* 11 (2020), 953.
- [96] E. Riba, D. Mishkin, D. Ponsa, E. Rublee, and G. Bradski. 2020. Kornia: an Open Source Differentiable Computer Vision Library for PyTorch. In *Winter Conference on Applications of Computer Vision*. <https://arxiv.org/pdf/1910.02190.pdf>
- [97] Robin Rombach, Andreas Blattmann, Dominik Lorenz, Patrick Esser, and Björn Ommer. 2022. High-resolution image synthesis with latent diffusion models. In *Proceedings of the IEEE/CVF Conference on Computer Vision and Pattern Recognition*. 10684–10695.
- [98] James A. Russell. 1980. A circumplex model of affect. *Journal of Personality and Social Psychology* 39 (1980), 1161–1178. <https://doi.org/10.1037/h0077714>
- [99] Hiroshi Sasaki, Chris G Willcocks, and Toby P Breckon. 2021. Unit-ddpm: Unpaired image translation with denoising diffusion probabilistic models. *arXiv preprint arXiv:2104.05358* (2021).
- [100] KR Scherer. 2001. *Appraisal processes in emotion: Theory, methods, research*. Oxford University Press.
- [101] Melanie Schreiner, Thomas Fischer, and Rene Riedl. 2021. Impact of content characteristics and emotion on behavioral engagement in social media: literature review and research agenda. *Electronic Commerce Research* 21 (2021), 329–345.
- [102] selfcontrolapp.com. [n. d.]. SelfControl. selfcontrolapp.com (Accessed: 08.07.2022).
- [103] Jaana Simola, Kevin Le Fevre, Jari Torniaainen, and Thierry Baccino. 2015. Affective processing in natural scene viewing: Valence and arousal interactions in eye-fixation-related potentials. *NeuroImage* 106 (2015), 21–33.
- [104] Jiaming Song, Chenlin Meng, and Stefano Ermon. 2020. Denoising diffusion implicit models. *arXiv preprint arXiv:2010.02502* (2020).
- [105] Eva Specker, Helmut Leder, Raphael Rosenberg, Lisa Mira Hegelmaier, Hanna Brinkmann, Jan Mikuni, and Hideaki Kawabata. 2018. The universal and automatic association between brightness and positivity. *Acta Psychologica* 186 (2018), 47–53.
- [106] Shabbir Syed-Abdul, Luis Fernandez-Luque, Wen-Shan Jian, Yu-Chuan Li, Steven Crain, Min-Huei Hsu, Yao-Chin Wang, Dorjsuren Khandregzen, Enkhzaya Chuluunbaatar, Phung Anh Nguyen, and Der-Ming Liou. 2013. Misleading Health-Related Information Promoted Through Video-Based Social Media: Anorexia on YouTube. *Journal of Medical Internet Research* 15, 2 (Feb. 2013), e2237. <https://doi.org/10.2196/jmir.2237>
- [107] Vincent W-S Tseng, Matthew L Lee, Laurent Denoue, and Daniel Avrahami. 2019. Overcoming distractions during transitions from break to work using a conversational website-blocking system. In *Proc. of the 2019 CHI conference on human factors in computing systems*.

- [108] Oshin Vartanian, Vinod Goel, Elaine Lam, Maryanne Fisher, and Josipa Granic. 2013. Middle temporal gyrus encodes individual differences in perceived facial attractiveness. *Psychology of Aesthetics, Creativity, and the Arts* 7, 1 (2013), 38.
- [109] Soroush Vosoughi, Deb Roy, and Sinan Aral. 2018. The spread of true and false news online. *Science* 359, 6380 (2018), 1146–1151. <https://doi.org/10.1126/science.aap9559>
- [110] Tengfei Wang, Ting Zhang, Bo Zhang, Hao Ouyang, Dong Chen, Qifeng Chen, and Fang Wen. 2022. Pretraining is all you need for image-to-image translation. *arXiv preprint arXiv:2205.12952* (2022).
- [111] Heekyung Yang, Jongdae Han, and Kyungha Min. 2020. Emotion variation from controlling contrast of visual contents through EEG-Based deep emotion recognition. *Sensors* 20, 16 (2020), 4543.
- [112] Kimberly Young. 2009. Understanding online gaming addiction and treatment issues for adolescents. *The American journal of family therapy* 37, 5 (2009), 355–372.
- [113] Jusheng Yu. 2014. We look for social, not promotion: Brand post strategy, consumer emotions, and engagement. *International Journal of Media & Communication* 1, 2 (2014), 28–37.
- [114] Lvmin Zhang and Maneesh Agrawala. 2023. Adding Conditional Control to Text-to-Image Diffusion Models. *arXiv preprint arXiv:2302.05543* (2023).
- [115] Yuxin Zhang, Nisha Huang, Fan Tang, Haibin Huang, Chongyang Ma, Weiming Dong, and Changsheng Xu. 2023. Inversion-based style transfer with diffusion models. In *Proceedings of the IEEE/CVF Conference on Computer Vision and Pattern Recognition*. 10146–10156.
- [116] Min Zhao, Fan Bao, Chongxuan Li, and Jun Zhu. 2022. Egsde: Unpaired image-to-image translation via energy-guided stochastic differential equations. *Advances in Neural Information Processing Systems* 35 (2022), 3609–3623.
- [117] Sicheng Zhao, Chuang Lin, Pengfei Xu, Sendong Zhao, Yuchen Guo, Ravi Krishna, Guiguang Ding, and Kurt Keutzer. 2019. Cycleemotiongan: Emotional semantic consistency preserved cyclegan for adapting image emotions. In *Proceedings of the AAAI conference on artificial intelligence*, Vol. 33. 2620–2627.
- [118] Sicheng Zhao, Xin Zhao, Guiguang Ding, and Kurt Keutzer. 2018. Emotiongan: Unsupervised domain adaptation for learning discrete probability distributions of image emotions. In *Proceedings of the 26th ACM international conference on Multimedia*. 1319–1327.
- [119] Jun-Yan Zhu, Taesung Park, Phillip Isola, and Alexei A Efros. 2017. Unpaired image-to-image translation using cycle-consistent adversarial networks. In *Proceedings of the IEEE international conference on computer vision*. 2223–2232.
- [120] Siqi Zhu, Chunmei Qing, Canqiang Chen, and Xiangmin Xu. 2022. Emotional Generative Adversarial Network for Image Emotion Transfer. *Expert Systems with Applications* (2022), 119485.

A DATASET

The integrated dataset shows the strong correlation between high and low valence with high arousal, commonly found in emotional ratings (see Figure 16).

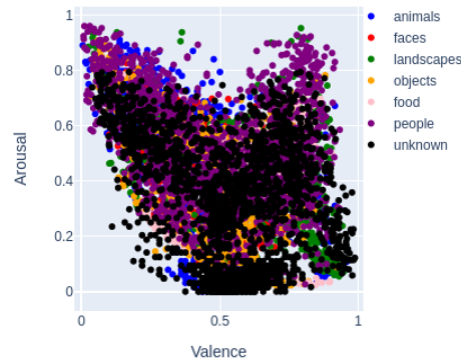


Fig. 16. Location of stimuli of our integrated dataset within the valence arousal space of the Circumplex Model of Affect [98].

B BACKGROUND: DIFFUSION MODELS

In this section, we adopt the notation of [81] for clarity. For a detailed derivation of diffusion denoising probabilistic models, we refer readers to [50].

Text-guided diffusion models map a random noise vector z_t and a textual condition \mathcal{P} to an output image z_0 , corresponding to the conditioning prompt. Sequential denoising is performed by training a network ϵ_θ to predict artificial noise, with the objective:

$$\min_{\theta} \mathbb{E}_{z_0, \epsilon \sim \mathcal{N}(0, I), t \sim \text{Uniform}(1, T)} \|\epsilon - \epsilon_\theta(z_t, t, C)\|^2. \quad (1)$$

$C = \psi(\mathcal{P})$ is the embedding of the text condition, and z_t is a noised version of the sampled data z_0 at time step t . During inference, starting from a noise vector z_T , noise is progressively removed over T steps using the trained network.

As we intend to introduce subtle changes to a given real image, we employ deterministic DDIM sampling [104]:

$$z_{t-1} = \frac{\alpha_{t-1}}{\alpha_t} z_t + \left(\sqrt{\frac{1}{\alpha_{t-1}} - 1} - \sqrt{\frac{1}{\alpha_t}} \right) \cdot \epsilon_\theta(z_t, t, C). \quad (5)$$

For the definition of α_t see Section B.1.

Diffusion models can operate in image pixel space, with z_0 representing a real image sample. In our work, we utilize the SDXL model [91], where the forward diffusion process is applied to a latent image encoding $z_0 = E(I)$, and an image decoder is used at the end of the reverse diffusion process to produce $I = D(z_0)$.

B.1 Forward diffusion process

The forward diffusion process is presented here for completeness and can be defined as follows:

$$z_t = \sqrt{\alpha_t} z_0 + \sqrt{1 - \alpha_t} \cdot \epsilon, \quad \epsilon \sim \mathcal{N}(0, I), \quad (6)$$

where $\alpha_t = \prod_{i=1}^t (1 - \beta_i)$ is the cumulative product of the noise schedule and $\beta = \{\beta_1, \beta_2, \dots, \beta_T\}$ is the noise schedule controlling the diffusion process. $\epsilon \sim \mathcal{N}(0, I)$ represents Gaussian noise sampled at each step.

B.2 Classifier guidance

To improve control and precision during the denoising process, classifier guidance was proposed as a post-hoc conditioning mechanism for diffusion models [35]. This method modifies the noise prediction process by incorporating a gradient term derived from a classifier $p_\phi(y|z_t)$, where y denotes the conditioning input:

$$\hat{\epsilon}_\theta(z_t, t, C, y) = \epsilon_\theta(z_t, t, C) + s \cdot \nabla_{z_t} \log p_\phi(y|z_t). \quad (7)$$

Here, $\epsilon_\theta(z_t, t)$ is the original noise prediction, s is a guidance scale parameter that controls the strength of the classifier’s influence, and $\nabla_{z_t} \log p_\phi(y|z_t)$ denotes the gradient of the log-probability of y with respect to z_t . By incorporating the classifier’s gradient, the denoising process is guided towards samples that better match the desired conditioning y .

B.3 Classifier-free guidance

Another approach that offers posthoc conditional control over the denoising process is classifier-free guidance (CFG) [51]. It enhances the effect of conditioned text by combining an additional unconditional prediction with the conditioned prediction through extrapolation. Formally, let $\emptyset = \psi(\text{""})$ represent the embedding of a null text, and let w denote the guidance scale parameter. The classifier-free guidance prediction is given by:

$$\hat{\epsilon}_\theta(z_t, t, C, \emptyset) = w \cdot \epsilon_\theta(z_t, t, C) + (1 - w) \cdot \epsilon_\theta(z_t, t, \emptyset). \quad (8)$$

B.4 DDIM inversion

DDIM inversion [35, 104] offers a straightforward approach to reverse DDIM sampling based on the assumption that the ODE process can be reversed with sufficiently small steps. The inversion process is described by:

$$z_{t+1} = \frac{\alpha_{t+1}}{\alpha_t} z_t + \left(\sqrt{\frac{1}{\alpha_{t+1}} - 1} - \sqrt{\frac{1}{\alpha_t}} \right) \cdot \epsilon_\theta(z_t, t, C). \quad (9)$$

Essentially, the diffusion process is reversed, transitioning from $z_0 \rightarrow z_T$ rather than the forward process of $z_T \rightarrow z_0$, where z_0 represents the encoding of the given real image.

B.5 Null-text optimization

Null-text optimization (NTO) [81] addresses the issue of DDIM inversion with CFG leading to visual artifacts and reduced editability of the inverted noise vector. NTO initializes $\tilde{z}_T = z_T^*$ using the sequence of noisy latent codes z_T^*, \dots, z_0^* produced by DDIM inversion, where $z_0^* = z_0$. It then optimizes the timestamps $t = T, \dots, 1$ with a fixed guidance scale (e.g., $w = 7.5$) by minimizing:

$$\min_{\theta_t} \|z_{t-1}^* - z_{t-1}(\tilde{z}_t, \theta_t, C)\|^2. \quad (3)$$

Here, $z_{t-1}(\tilde{z}_t, \theta_t, C)$ denotes a DDIM sampling step using \tilde{z}_t , the unconditional embedding θ_t , and the conditional embedding C . At each step, \tilde{z}_{t-1} is updated as $\tilde{z}_{t-1} = z_{t-1}(\tilde{z}_t, \theta_t, C)$. With the optimized noise $\tilde{z}_T = z_T^*$ and unconditional embeddings $\{\theta_t\}_{t=1}^T$, the input image can be de-noised while retaining editability.

C ADDITIONAL QUALITATIVE RESULTS FROM THE CRITERIA ALIGNMENT EXPERIMENT

Figures 17, 18, and 19 show further qualitative results of the criteria alignment experiment.

D ADDITIONAL QUALITATIVE RESULTS FROM THE BIDIRECTIONAL CHANGES EXPERIMENT

Figure 20 shows additional qualitative results from the bidirectional emotional changes experiment.

E ADDITIONAL ADAPTED SOCIAL MEDIA IMAGES

Figures 21 and 22 show further examples of adapted images used in the social media study.

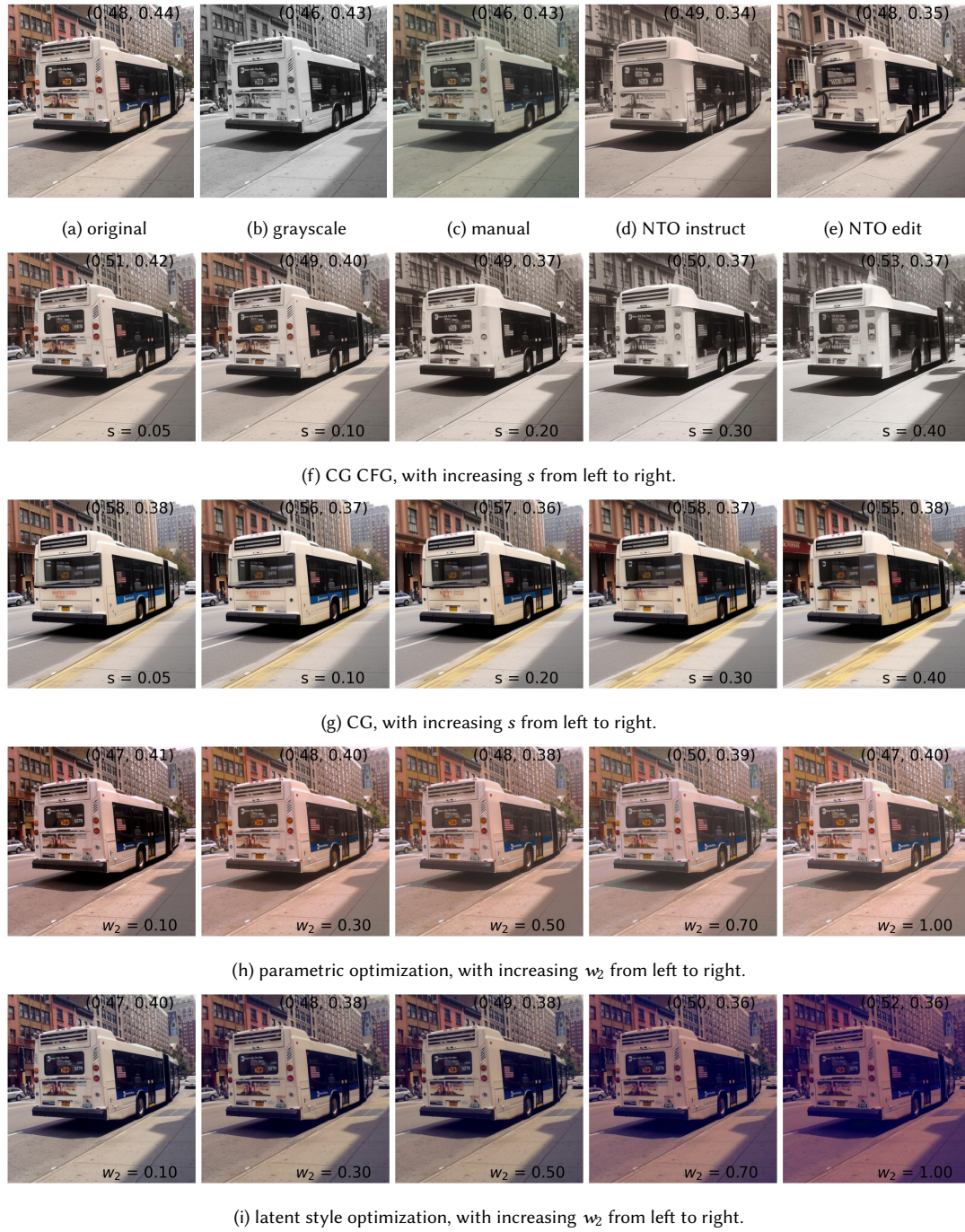


Fig. 17. Example result of COCO. Image caption: "A double city bus is pulled up to a bus stop."



Fig. 18. Example result of COCO. Image caption: "A woman holding a phone in one hand up to her ear."

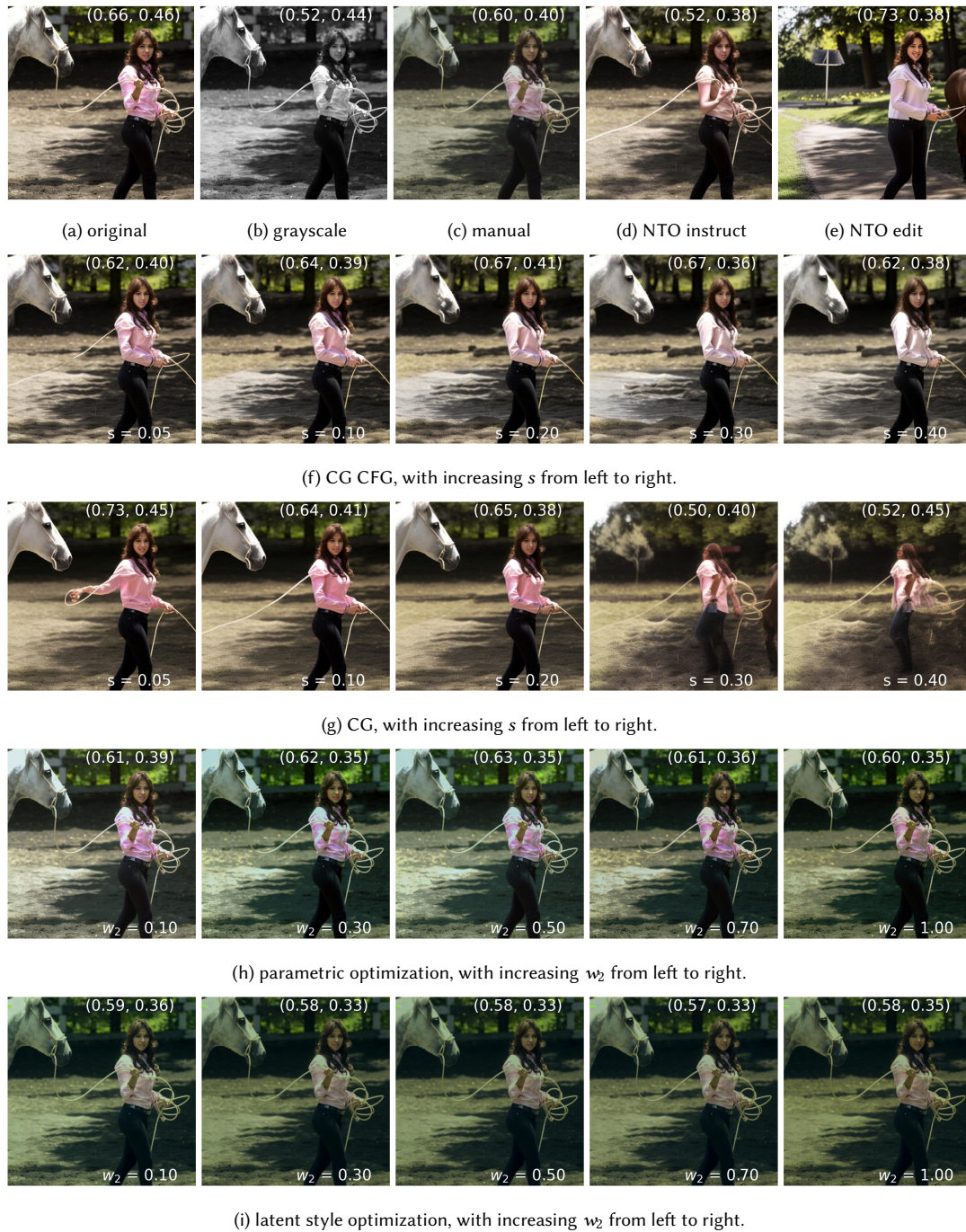


Fig. 19. Example result of COCO. Image caption: "A woman walking a horse on some property with trees."



Fig. 20. Example result of bidirectional emotional change analysis. The emotional reference is displayed in the bottom-right corner, while the inferred valence and arousal values are shown in the top-right corner. Image caption: "Two women in athletic wear posing outdoors near a body of water."



(a) Subjects get older. Image caption: "A woman in athletic wear sits on a bed holding a mug with a packet of FITWHEY protein powder beside her."



(b) Subjects decline in attractiveness. Image caption: "Two individuals standing close to each other in a room with framed artwork."



(c) Subjects get clothed. Image caption: "A woman in a striped bikini stands in front of a modern white building with balconies and glass railings."



(d) Subjects' facial expression is changed. Image caption: "'Bride and groom in traditional attire in front of a fountain'"

Fig. 21. Social media images adapted using style optimization, original, parametric optimization, and CG & CFG (from left to right). Each image is representative for a type of change commonly induced through the CG & CFG diffusion algorithm (see sub-caption).



(a) Subjects get removed. Image caption: "Hand holding a single yellow flower with a person standing in a field in the background."



(b) Subjects are reduced in size. Image caption: "A dog standing on a rocky ledge above a small waterfall in a forest."



(c) Animals appear less cute. Image caption: "A woman running on the beach with a dog on a leash."



(d) Background becomes simpler. Image caption: "A person in a red shirt jumps joyfully among string lights at night in a garden."

Fig. 22. Social media images adapted using style optimization, original, parametric optimization, and CG & CFG (from left to right). Each image is representative for a type of change commonly induced through the CG & CFG diffusion algorithm (see sub-caption).